Title

BOLA (BolA Family Member 3) Deficiency Controls Endothelial Metabolism and Glycine Homeostasis in Pulmonary Hypertension

Journal

Circulation, 139(19)

ISSN

0009-7322

Authors

Yu, Qiujun
Tai, Yi-Yin
Tang, Ying
et al.

Publication Date

2019-05-07

DOI

10.1161/circulationaha.118.035889

Peer reviewed

Published in final edited form as:

Circulation. 2019 May 07; 139(19): 2238–2255. doi:10.1161/CIRCULATIONAHA.118.035889.

BOLA3 deficiency controls endothelial metabolism and glycine homeostasis in pulmonary hypertension

Qiujun Yu, MD, PhD[1], **Yi-Yin Tai, MS**[1], **Ying Tang, MS**[1], **Jingsi Zhao, MS**[1], **Vinny Negi, PhD**[1], **Miranda K. Culley, BA**[1], **Jyotsna Pilli, PhD**[1], **Wei Sun, MD**[1], **Karin Brugger, MD**[2], **Johannes Mayr, MD**[2], **Rajeev Saggar, MD**[3], **Rajan Saggar, MD**[4], **W. Dean Wallace, MD**[4], **David J. Ross, MD**[4], **Aaron B. Waxman, MD, PhD**[5], **Stacy G. Wendell, PhD**[6,7], **Steven J. Mullett, BS**[7], **John Sembrat, BS**[1], **Mauricio Rojas, MD**[1], **Omar F. Khan, PhD**[8], **James E. Dahlman, PhD**[9], **Masataka Sugahara, MD**[1], **Nobuyuki Kagiyama, MD**[1], **Taijyu Satoh, MD**[1], **Manling Zhang, MD, MS**[1], **Ning Feng, MD, PhD**[1], **John Gorcsan III, MD**[10], **Sara O. Vargas, MD**[11], **Kathleen J. Haley, MD**[10], **Rahul Kumar, PhD**[12], **Brian B. Graham, MD**[12], **Robert Langer, ScD**[8,13], **Daniel G. Anderson, PhD**[8,13], **Bing Wang, MD, PhD**[14], **Sruti Shiva, PhD**[1], **Thomas Bertero, PhD**[15], and **Stephen Y. Chan, MD, PhD**[1]

[1]Center for Pulmonary Vascular Biology and Medicine, Center for Metabolism and Mitochondrial Medicine, Pittsburgh Heart, Lung, Blood, and Vascular Medicine Institute, Division of Cardiology and Division of Pulmonary and Critical Care Medicine, Department of Medicine, University of Pittsburgh School of Medicine and University of Pittsburgh Medical Center, Pittsburgh, PA

[2]Department of Pediatrics, Paracelsus Medical University Salzburg, Salzburg, Austria

[3]Department of Medicine, University of Arizona, Phoenix, AZ

[4]Departments of Medicine and Pathology, David Geffen School of Medicine, University of California, Los Angeles, Los Angeles, CA

[5]Division of Pulmonary and Critical Care Medicine, Department of Medicine, Brigham and Women's Hospital, Harvard Medical School, Boston, MA

[6]Department of Pharmacology and Chemical Biology, University of Pittsburgh, Pittsburgh, PA

[7]Health Sciences Metabolomics and Lipidomics Core, University of Pittsburgh, Pittsburgh, PA

[8]Department of Chemical Engineering, Massachusetts Institute of Technology, Cambridge, MA

[9]Wallace H. Coulter Department of Biomedical Engineering, Georgia Institute of Technology, Atlanta, GA

[10]Division of Cardiology, Department of Medicine, Washington University in St. Louis, St. Louis, MO

[11]Department of Pathology, Boston Children's Hospital, Boston, MA

Corresponding Author: Stephen Y. Chan, MD, PhD, Center for Pulmonary Vascular Biology and Medicine, Pittsburgh Heart, Lung, Blood, and Vascular Medicine Institute, Division of Cardiology, Department of Medicine, University of Pittsburgh Medical Center, 200 Lothrop Street BST1704.2, Pittsburgh, PA USA 15261, Tel: 412-383-6990, Fax: 412-624-9160, chansy@pitt.edu.

Disclosures

S.Y.C. has served as a consultant for Zogenix (Significant) and Vivus (Modest) and holds research grants for Pfizer and Actelion. The authors declare no other conflicts of interest.

[12]Program in Translational Lung Research, University of Colorado, Denver, Aurora, CO

[13]David H. Koch Institute for Integrative Cancer Research, Massachusetts Institute of Technology, Cambridge, MA

[14]Molecular Therapy Lab, Stem Cell Research Center, University of Pittsburgh School of Medicine, Pittsburgh, PA

[15]Université Côte d'Azur, CNRS, UMR7284, INSERM U1081, Institute for Research on Cancer and Aging, Nice (IRCAN), Nice, France

Abstract

Background—Deficiencies of iron-sulfur (Fe-S) clusters, metal complexes that control redox state and mitochondrial metabolism, have been linked to pulmonary hypertension (PH), a deadly vascular disease with poorly defined molecular origins. The BolA Family Member 3 (BOLA3) regulates Fe-S biogenesis, and mutations in BOLA3 result in multiple mitochondrial dysfunction syndrome, a fatal disorder associated with PH. The mechanistic role of BOLA3 in PH remains undefined.

Methods—In vitro assessment of BOLA3 regulation and gain and loss of function assays were performed in human pulmonary artery endothelial cells (PAECs) using siRNA and lentiviral vectors expressing the mitochondrial isoform of BOLA3. Polymeric nanoparticle 7C1 was utilized for lung endothelial-specific delivery of BOLA3 siRNA oligonucleotides in mice. Overexpression of pulmonary vascular BOLA3 was performed by orotracheal transgene delivery of adeno-associated virus in mouse models of PH.

Results—In cultured hypoxic PAECs as well as lung from human Group 1 and 3 PH patients as well as multiple rodent models of PH, endothelial BOLA3 expression was down-regulated, which involved HIF-2α-dependent transcriptional repression via HDAC-mediated histone deacetylation. In vitro gain and loss of function studies demonstrated that BOLA3 regulated Fe-S integrity, thus modulating lipoate-containing 2-oxoacid dehydrogenases with consequent control over glycolysis and mitochondrial respiration. In contexts of siRNA knockdown and naturally occurring human genetic mutation, cellular BOLA3 deficiency down-regulated the glycine cleavage system protein H (GCSH), thus bolstering intracellular glycine content. In the setting of these alterations of oxidative metabolism and glycine levels, BOLA3 deficiency increased endothelial proliferation, survival, and vasoconstriction, while decreasing angiogenic potential. In vivo, pharmacologic knockdown of endothelial BOLA3 and targeted overexpression of BOLA3 in mice demonstrated that BOLA3 deficiency promotes histologic and hemodynamic manifestations of PH. Notably, the therapeutic effects of BOLA3 expression were reversed by exogenous glycine supplementation.

Conclusions—BOLA3 acts as a crucial lynchpin connecting Fe-S-dependent oxidative respiration and glycine homeostasis with endothelial metabolic re-programming critical to PH pathogenesis. These results provide a molecular explanation for the clinical associations linking PH with hyperglycinemic syndromes and mitochondrial disorders. These findings also identify novel metabolic targets, including those involved in epigenetics, iron-sulfur biogenesis, and glycine biology, for diagnostic and therapeutic development.

Keywords

Pulmonary hypertension; iron-sulfur cluster; mitochondria; glycine; endothelial

Introduction

Pulmonary hypertension (PH), its severe subtype pulmonary arterial hypertension (PAH or World Health Organization Group 1 PH), and its subtype characterized by hypoxic lung diseases (WHO Group 3 PH) are enigmatic vascular diseases characterized by profound metabolic re-programming in multiple vascular cell types, often driven by the master transcription factors of hypoxia, hypoxia inducible factors (HIF)-1α and HIF-2α. We and others have explored the pathogenic impact of mitochondrial dysfunction in the pulmonary arterial endothelial cells (PAECs) [1], but the full relevance of this principle to PH has been incompletely defined.

We previously reported that hypoxia decreased the iron-sulfur (Fe-S) cluster assembly proteins ½ (ISCU½) [2], which are essential for Fe-S cluster biogenesis. Fe-S clusters ([4Fe-4S] and [2Fe-2S]) are bioinorganic prosthetic groups that mediate electron transport and cellular redox processes [3]. We found that down-regulation of ISCU½ decreased Fe-S dependent mitochondrial respiration and promoted glycolysis (Warburg-like effect seen in cancer cells). Chronic repression of ISCU½, particularly in PAECs, drove pulmonary vascular remodeling and PH [4].

Beyond ISCU½, Fe-S biogenesis in human cells is controlled by a conserved set of over 30 assembly proteins [3]. Rare mutations in the Fe-S scaffold protein BOLA3 (BolA Family Member 3) [5, 6] are an underlying cause of a fatal autosomal recessive disorder, multiple mitochondrial dysfunction syndrome subtype 2 (MMDS2). A manifestation of MMDS includes PH [7, 8], accompanied by emerging links (reported by the Uniprot Consortium) with BOLA3 mutations [9]. BOLA3 is crucial in the mitochondria for Fe-S maturation downstream of ISCU½ [10]. BOLA3 also controls Fe-S-dependent synthesis of lipoic acid, via facilitating Fe-S clusters to act as sulfur donors for lipoate [11]. Lipoate is transferred as a covalent moiety to lysine residues of multiple mitochondrial enzymes, including the E2 subunits of pyruvate dehydrogenase (PDH), thus affecting oxidative metabolism [12]. The mitochondrial H protein of the glycine cleavage system (GCSH), also depends upon lipoate modification for modulation of glycine production and cellular homeostasis of this amino acid. Importantly, glycine levels are critical mediators of cellular proliferative capacity and are an overarching regulator of growth in cancer cells [13]. However, glycine and its links to Fe-S biology have not been explored in pulmonary vascular disease. Thus, we endeavored to determine whether BOLA3 and its effects on both Fe-S-specific oxidative respiration as well as the glycine cleavage system in pulmonary arterial endothelium are key pathogenic drivers in multiple forms of PH.

Materials and Methods

The materials and methods that support the study findings are available from the corresponding author on reasonable request. Several approaches were used in this study: *in*

situ staining of human and rodent PH lungs, *in vitro* studies of cultured primary cells, and *in vivo* studies of PH mice where the consequences of manipulating BOLA3 and glycine levels were investigated. The corresponding author had access to all data and takes responsibility for the integrity and data analysis. Detailed description of *Materials and Methods* is provided in the Online Data Supplement.

Human and animal subjects and ethical considerations

Tables S1–S2 describe human PH specimens, and non-PH human lung specimens were described previously [14]. Procedures were approved by institutional review boards at Partners Health Care, the University of California, Los Angeles, Boston Children's Hospital, the University of Pittsburgh, and the New England Organ Bank. Ethical approval and informed consent conformed to the Declaration of Helsinki. All animal experiments were approved by the University of Pittsburgh (DLAR).

Statistical analysis

Data are represented as mean ± SEM or mean ± SD. For cell culture data, 3 independent experiments were performed in triplicate. Animal numbers were calculated to measure ≥ 20% difference between means of experimental and control groups with power of 80% and SD of 10%. Normality of data was confirmed by Shapiro Wilk testing. For comparisons between two groups, a 2-tailed Student's *t* test was used for normally distributed data. For comparisons among groups, one-way or two-way ANOVA and *post-hoc* Tukey testing was performed. A P-value less than 0.05 was considered significant.

Results

BOLA3 expression is hypoxia-dependent and down-regulated in pulmonary vascular endothelial cells in PH

In human and rodent models of PH where HIF-1α and HIF-2α are known to be active, BOLA3 expression was reduced within endothelial and smooth muscle cells of small diseased pulmonary arterioles in human PAH (Table S1, Figure 1A) and Group 3 PH with idiopathic pulmonary fibrosis (IPF) (Table S2, Figure 1B). Similarly, in inflammatory and hypoxic PH mice relevant to Group 1 and Group 3 PH, pulmonary BOLA3 was decreased in wildtype mice suffering from hypoxic PH (Figure 1C–D,S1A), and in mice harboring a pulmonary specific transgene expressing the inflammatory cytokine interleukin-6 (IL-6) [15], with or without hypoxia (Figure 1C). Pulmonary vascular BOLA3 (Figure S1A,E) was decreased in mice suffering from a variant model [16] of severe fibrotic lung disease induced by exposure to bleomycin and hypoxia (Figure S1). Female PH mice displayed similar decreases of BOLA3 via exposure to hypoxia alone or hypoxia + bleomycin (Figure S1E). Decreases of BOLA3 were observed in inflammatory models of PH, such as chronic *S. mansoni* infection in mice (Figure 1E), monocrotaline exposure (Figure 1F,S2A) and SU5416+hypoxic exposure in rats (Figure S2B). BOLA3 downregulation was observed in CD31-positive endothelial cells from diseased vs. control lungs of hypoxic PH mice (Figure 1G). Correspondingly, we found that hypoxia down-regulated BOLA3 in cultured PAECs (Figure 1H–I). BOLA3 transcript in cultured PAECs was not affected by all inflammatory cytokines or deficiency of factors genetically associated with PH (Figure S2C–D).

Interestingly, while BOLA3 was decreased in diseased PA smooth muscle cells (PASMCs) *in situ* (Figure 1), BOLA3 expression in cultured PASMCs was not altered by hypoxia (Figure S2E), suggesting at least partial predilection of this biology for endothelial cells. Also considering the importance of ISCU½ in endothelial cells to drive PH [2, 4], we focused on studying BOLA3 in PAECs.

Hypoxia represses BOLA3 transcription via a HIF-2α-HDAC-dependent epigenetic axis

We concentrated on the roles of HIF-1α and HIF-2α in driving endothelial BOLA3 downregulation in hypoxia. Knockdown of HIF-2α -- but not HIF-1α -- partially rescued BOLA3 in hypoxic PAECs (Figure 2A), and overexpression of constitutively active HIF-2α in normoxic PAECs reduced BOLA3 (Figure 2B). Although no HIF-2α binding site was predicted in the BOLA3 promoter, two sites (A/B) were predicted as histone binding sites and thus modulated by lysine 9 acetylation of histone 3 (H3K9) (Figure 2C). Chromatin immunoprecipitation (ChIP) was performed in PAECs to pull down acetylated H3K9, coupled with PCR of ChIP contents (Table S3) to detect these BOLA3 promoter sites. Binding of sites A and B with complexes containing acetylated H3K9 proteins was decreased in hypoxia or with forced expression of constitutive HIF-2α (Figure 2C), indicating a more closed chromatin state at these sites less conducive to active transcription compared with normoxia. In hypoxic PAECs, BOLA3 expression was rescued with enhanced histone acetylation via inhibition by HDAC1 siRNA or the HDAC inhibitor valproic acid (Figure 2D–G). While HDAC1 expression was unchanged under hypoxia (Figure 2H), HDAC1 knockdown enhanced enrichment of acetylated H3K9 at the BOLA3 promoter both in hypoxia (Figure 2I) and during HIF-2α expression (Figure 2J). By ChIP-PCR pulldown of HDAC1, HDAC1 binding was enriched at the BOLA3 promoter sites (Figure 2K). However, HIF-2α did not affect that binding, indicating that the role of HDAC1 on H3K9 acetylation at these sites is more complex and does not rely upon altered HDAC1 expression or binding. Thus, the down-regulation of BOLA3 expression in hypoxia depends in large part upon HIF-2α activity coupled with epigenetic control of H3K9 promoter acetylation.

BOLA3 controls Fe-S integrity and lipoate-dependent activity of the mitochondrial enzyme PDH

To determine whether BOLA3 controls Fe-S levels in PAECs, we utilized a fluorescent quantitative detection system of intracellular [2Fe-2S] clusters dependent upon glutaredoxin 2 (GRX2) protein homodimerization as described [4]. Consistent lentiviral sensor delivery was confirmed in cells undergoing BOLA3 siRNA knockdown vs. scramble control (Figure S3). While fluorescent signal was unchanged with non-Fe-S-dependent sensors (GCN4), BOLA3 knockdown reduced GRX2 fluorescence (Figure 3A), reflecting a down-regulation of Fe-S levels. Moreover, BOLA3 knockdown modestly decreased expression of components of Fe-S-dependent mitochondrial Complex I (NDUFV2) and II (SDHB), leading to Complex I activity repression in normoxia and hypoxia (Figure 3B,D). Conversely, forced BOLA3 expression in hypoxia via lentiviral transgene delivery rescued NDUFV2, SDHB, and Complex I activity (Figure 3C,E). Thus, BOLA3 directly controls Fe-S integrity and mitochondrial complex protein levels to regulate respiratory complex activity in PAECs.

Beyond regulating Fe-S integrity, BOLA3 has been reported to control the Fe-S-dependent generation of lipoate, a sulfur-containing moiety and post-translational modification crucial to some metabolic enzymes [12] such as pyruvate dehydrogenase (PDH). In PAECs, we also found that the lipoate-modified form of PDH was down-regulated by BOLA3 inhibition, accompanied by concomitant decrease in PDH enzymatic activity (Figure 3F–G). Conversely, lipoylated PDH and PDH activity were rescued in hypoxia by forced BOLA3 expression (Figure 3I–J). As expected from the known consequences of inhibiting PDH, BOLA3 knockdown increased glycolytic enzymes [including lactate dehydrogenate (LDHA) and pyruvate dehydrogenase kinase1 (PDK1), Figure 3H], while forced BOLA3 expression reversed changes in these gene networks in hypoxia (Figure 3K). Notably, phosphorylation of PDK1 was also up-regulated by BOLA3 knockdown (Figure S4A), which would specifically reinforce the inhibition of activity of non-lipoylated PDH. Correspondingly, exposure to dichloroacetate (DCA), a PDK phosphorylation inhibitor tested therapeutically in PAH [17], partially reversed the reduction of PDH activity with BOLA3 knockdown (Figure S4B), consistent with the notion that DCA can overcome the weakened interaction of PDK with PDH induced by lipoate deficiency [18]. Thus, along with its role in Fe-S synthesis, BOLA3 carries an essential role in controlling genes critical for endothelial glycolysis and lipid synthesis, stemming at least partially via control of lipoate modifications of PDH.

BOLA3 deficiency activates glycine production by up-regulating the glycine cleavage system protein H (GCSH)

We hypothesized that the control of lipoate synthesis by BOLA3 would influence other lipoate-dependent enzymes such as the glycine cleavage system protein H (GCSH), a protein that catabolizes glycine. Consistent with the down-regulation of lipoate synthesis (Figure 3F), BOLA3 knockdown in PAECs down-regulated GCSH (Figure 4A) and increased intracellular glycine content in normoxia (Figure 4B), thus phenocopying the effects of hypoxia on glycine in PAECs (Figure 4B) and in other cancer cells [19]. Conversely, forced BOLA3 expression reduced glycine accumulation in hypoxia by upregulating GCSH (Figure 4C–D). High resolution liquid chromatography mass spectrometry (LC-HRMS) of metabolite levels resulting after BOLA3 knockdown confirmed increased glycine as well as relevant downstream metabolites serine and sarcosine which would be expected to increase consequent to high glycine (Figure 4E–F). Neither glycine dehydrogenase (GLDC), a subunit in the glycine cleavage enzyme, nor serine hydroxymethyltransferase (SHMT1), which catalyzes reversible conversion of serine to glycine, were altered with BOLA3 knockdown (Figure S5A). Furthermore, GCSH knockdown (Figure S5B) up-regulated glycine, most prominently during hypoxia but less substantially in normoxia (Figure 4G), suggesting that overall hypoxic reprogramming provided a permissive environment that allows BOLA3 deficiency and its downstream down-regulation of GCSH to carry their most robust effects on glycine. With either BOLA3 knockdown (Figure S5H) or endogenous BOLA3 deficiency in hypoxia (Figure 4H), forced GCSH expression (Figure S5C) reversed the elevation of glycine, thus establishing the essential role of GCSH in mediating the effects of BOLA3 deficiency on glycine metabolism. Finally, this decreased lipoylation activity, decreased GCSH, and increased glycine production as driven by BOLA3 deficiency in PAECs was phenocopied in primary fibroblasts derived from a MMDS2 patient carrying

homozygous missense mutations in BOLA3 [6] (Figure S6), thus revealing the relevance of these findings to the inherited predisposition to PH in these patients.

Elevation of glycine has been linked to cancer cell proliferation and increased glycolysis in ischemia and hypoxia [13, 20]. Correspondingly, in hypoxia, exogenous glycine augmented increases of glycolytic enzymes LDHA and PDK1 (Figure S5D–E) and promoted PAEC proliferation (Figure S5F–G), phenocopying the effects of GCSH knockdown (Figure 4I–J, M–N). GCSH reversed increases of LDHA and PDK1 during hypoxia (Figure 4K–L) and siRNA-induced BOLA3 knockdown (Figure S5I–J). Consequently, GCSH reversed, at least partially, the changes in multiple functional indices of oxidative metabolism, including the decreases of mitochondrial Complex I and PDH activity induced by BOLA3 deficiency (Figure S5K–L). Together, these data demonstrate that BOLA3 deficiency increases glycine via downregulation of GCSH, influencing additive pathobiology beyond the effects of Fe-S deficiency on glucose metabolism.

BOLA3 deficiency activates PAEC glycolysis and fatty acid oxidation and drives the production of reactive oxygen species

Based on these alterations of metabolic gene expression and enzyme activity, we determined whether BOLA3 deficiency modulates endothelial respiration. Via extracellular flux analysis, oxygen consumption rate (OCR) and extracellular acidification rate (ECAR, a marker of glycolysis) in cultured PAECs were assessed, with or without expression of a constitutively active form of HIF-2α to down-regulate BOLA3 and mimic the metabolic reprogramming of hypoxia. HIF-2α increased ECAR and basal glycolysis, an effect phenocopied by BOLA3 knockdown in normoxia alone (Figure S7A,C,E). BOLA3 knockdown in the presence of HIF-2α further promoted basal glycolysis. As expected, HIF-2α decreased basal OCR (Figure S7B,D). Surprisingly, BOLA3 knockdown, either in normoxia or with constitutive HIF-2α expression, increased basal and maximal OCR. To reconcile this observation with the Pasteur effect that shunts glucose away from oxidative phosphorylation, we hypothesized that BOLA3 deficiency mobilizes fatty acid flux and fatty acid oxidation (FAO) to increase oxygen consumption, despite the decreased, but not entirely absent, reservoir of Fe-S-dependent mitochondrial activity. Correspondingly, when fatty acid uptake was inhibited by etomoxir, a carnitine palmitoyl transferase (CPT1A) inhibitor, BOLA3 knockdown still drove increased basal glycolysis (Figure S7F,H) but decreased oxygen consumption (Figure S7G,I). While not appearing to alter crucial mitochondrial biogenesis genes (Figure S7J–K), such knockdown increased levels of CPT1A, the target of etomoxir (Figure S7L–M), indicating the ability to handle augmented FA flux through oxidative phosphorylation. When the fatty acid palmitate was used as the primary endothelial oxidative phosphorylation substrate, OCR was increased with BOLA3 knockdown but was reversed with etomoxir (Figure S7N). Together, these findings demonstrate that BOLA3 deficiency induces a metabolic shift towards glycolysis but, independent of the Pasteur effect, such deficiency shunts additional fatty acids for oxidative phosphorylation to blunt the overall decrease of OCR in hypoxia.

Considering this increase of endothelial respiration in the absence of fully functioning mitochondrial electron transport, we postulated that oxygen consumption induced by BOLA

deficiency must result in a profound oxidative state and mitochondrial generation of reactive oxygen species (ROS). Correspondingly, proton leak from the mitochondrial electron transport chain was increased by BOLA3 knockdown (Figure S8A). Mitosox red labelling of mitochondrial ROS (Figure S8B–C) and Amplex red labelling of hydrogen peroxide (Figure S8D) revealed that BOLA3 deficiency increased mitochondrial ROS in PAECs in normoxia; hypoxic increases of ROS were further exaggerated by BOLA3 knockdown. Oxidative stress with BOLA3 knockdown was also reflected by an increase in 8-oxoguanine, an oxidative damage product of guanine (Figure S8E). Conversely, BOLA3 overexpression reduced ROS production in hypoxia (Figure S8F–H). Taken together, BOLA3 deficiency promotes glycolysis in lieu of glucose-driven oxidative phosphorylation yet still bolsters oxygen consumption even in hypoxia by activating fatty acid oxidation and mitochondrial ROS generation.

BOLA3 deficiency reprograms PAECs to control proliferation, apoptosis, angiogenesis, and generation of vasoconstrictive factors

Downstream of Fe-S-dependent and glycine-dependent metabolic reprogramming events, we found that BOLA3 deficiency drives key phenotypic changes to promote endothelial activation and dysfunction. BOLA3 knockdown activated PAECs in normoxia and hypoxia increasing proliferative potential (Figure 5A,S9A) and decreasing apoptotic signaling (Figure 5B). Conversely, forced expression of BOLA3 in hypoxia decreased proliferation (Figure 5C) and increased apoptotic caspase activity (Figure 5D), thus revealing that BOLA3 deficiency blunts the pro-apoptotic hypoxic state and acts to maintain proliferation close to normoxic levels. BOLA3 deficiency also decreased angiogenic tube formation potential *in vitro* (Figure 5E–F) as well as *in vivo* angiogenesis by matriplug assay (Figure S9B–C). This was accompanied by repressing expression of the angiogenic factor VEGF (Figure 5G). Furthermore, BOLA3 overexpression stimulated angiogenic tube formation in hypoxia (Figure 5H). Finally, human PASMCs cultured in gel were overlaid with conditioned media from normoxic or hypoxic PAECs previously exposed to BOLA3 siRNA or control. As assessed by gel contraction, PASMC contraction was increased by media from BOLA3-deficient PAECs in normoxia and, more so, in hypoxia (Figure 5I), consistent with increased vasoconstrictor endothelin-1 (ET-1, Figure 5J) and decreased endothelial nitric oxide synthase (NOS3, Figure 5K) in PAECs. Forced BOLA3 expression in PAECs reduced PASMC contraction (Figure 5L), decreased ET-1, and increased NOS3 (Figure 5M–N). Importantly, consistent with proliferative effects of glycine in cancer cells [13], forced expression of GCSH blunted proliferation and increased production of ET-1 driven by BOLA3 deficiency. It did not reverse the decrease of apoptotic caspase activity, a pathophenotype possibly more dependent on Fe-S-dependent mitochondrial function than glycine production (Figure S9D–F). To ensure specificity of BOLA3 and GCSH knockdown, a second set of siRNAs were used to confirm key findings (Figure S10). Taken together, these data demonstrate that BOLA3 deficiency, dependent in part on its effects on GCSH, is both necessary and sufficient to promote a pro-proliferative and anti-apoptotic endothelial state, characterized by decreased angiogenesis and increased production of vasoconstrictive effectors.

Endothelial knockdown of BOLA3 dysregulates glycine metabolism and promotes hemodynamic and histologic manifestations of PH

Revealing the relevance of this BOLA3-dependent pathway in human PH, we found that pulmonary vascular lipoate and GCSH levels were down-regulated in Group 1 and Group 3 PH patients (Figure S11), consistent with the down-regulation of BOLA3 (Figure 1A–B). To demonstrate the importance of BOLA3 and its control of Fe-S-dependent and glycine-dependent mechanisms in PH, we assessed the *in vivo* consequences of repressing BOLA3 in the endothelium. To do so, we utilized the 7C1 nanoparticle intravenous system to serially deliver siRNAs across 4 weeks directly to the vascular endothelium of mice *in vivo* [21] (Figure 6A). A specific siRNA targeting murine BOLA3 (si-BOLA3) was screened for optimal efficiency of BOLA3 knockdown in cultured murine PAECs in Figure S12A. Detection of BOLA3 siRNA in pulmonary vascular CD31-positive endothelial cells after 4 weeks of treatment confirmed the successful delivery of the siRNA in 7C1 nanoparticle formulation (Figure S12B). While 7C1 offered efficient pulmonary endothelial delivery, dosing notably resulted in modest delivery in RV tissue (Figure S13A–B). Yet, such treatment did not significantly alter systemic vascular or left ventricular parameters (Figure S12D–H). Compared with control siRNA-treated mice (si-NC), mice administered BOLA3 siRNA demonstrated a selective reduction of BOLA3 in pulmonary vascular CD31-positive endothelial cells (Figure 6B, S12C). Furthermore, consistent with our *in vitro* findings, BOLA3 knockdown resulted in a concurrent downregulation of lipoate and GCSH expression in CD31+ (endothelial) cells (Figure 6C–D), thus increasing glycine content in mouse lung tissue (Figure 6E). In endothelial and vascular smooth muscle cells, BOLA3 knockdown increased proliferation marker PCNA and decreased apoptosis marker cleaved caspase 3 (Figure 6F–H). Consequently, pulmonary vascular remodeling (Figure 6I–K) and right ventricular systolic pressure (RVSP, Figure 6L) were increased. Right ventricular remodeling (Fulton index) was not significantly altered (Figure 6M). Nonetheless, when considering the vascular-specific effects of BOLA3, these data demonstrate that BOLA3 deficiency drives a combination of Fe-S-dependent and lipoate-dependent metabolic reprogramming in PAECs to promote pulmonary vascular proliferation and PH.

PH is prevented by overexpression of pulmonary vascular BOLA3 and is reversed by glycine supplementation

To investigate whether forced BOLA3 expression could rescue these PH pathophenotypes, mice received orotracheal administration of a recombinant adeno-associated virus (rAAV) carrying the BOLA3 transgene 4 weeks prior to a 3 week exposure to hypoxia (Figure 7A). rAAV was chosen for long term transgene delivery, as described [22], and serotype 6 was empirically selected for optimal endothelial delivery (Figure S14A). We confirmed that vector DNA (Figure S14B) and GFP reporter gene (Figure S14C–D) were present in mouse pulmonary vascular CD31-positive endothelial cells after 4 weeks post- AAV6 delivery. While modest rAAV6-BOLA3 expression was observed in RV tissue (Figure S13C–D), delivery did not affect systemic vascular or left ventricular parameters (Figure S14H–L). Rather, rAAV6-BOLA3 delivery increased BOLA3 in pulmonary vascular CD31-positive endothelial cells (Figures 7B, S14C,E). In these male chronically hypoxic mice, rAAV6-BOLA3 increased lipoate and GCSH levels in the pulmonary vasculature (Figure 7C–E) and reduced glycine accumulation in mouse lungs (Figure 7F). Correspondingly, rAAV6-

BOLA3 decreased proliferation marker PCNA and increased apoptosis marker cleaved caspase 3 in CD31+ (endothelial) and α-SMA+ (smooth muscle) pulmonary arteriolar cells in comparison with rAAV-GFP mice (Figure 7G–H). As a result, rAAV6-BOLA3 significantly decreased pulmonary arteriolar remodeling and muscularization (Figure 7I–J) as well as RVSP (Figure 7K) but not Fulton index (Figure 7L).

We aimed to determine whether forced BOLA3 expression could protect against PH across several mouse models with varying levels of hemodynamic severity (Figure 1): (1) female chronically hypoxic mice (Figure S15A); (2) male and female mice exposed to a combination of bleomycin and hypoxia (Figure S16–S17); and (3) chronically hypoxic male transgenic IL-6 mice [15] (Figure 8, S18A). As in male hypoxic mice, systemic hemodynamics were not affected by rAAV6-BOLA3 delivery (Figures S15I–J, S17G–J, S18D). In all cases, rAAV6-BOLA3 increased endothelial lipoate and GCSH (Figures S15B–C, S16B–C, S18B–C) and down-regulated PCNA (Figures S15D, S16D–E, 8A), thus decreasing pulmonary arteriolar remodeling (Figures S15E–F, S17A–B, 8B–C) and RVSP (Figures S15G; S17C,E; 8D). This was accompanied by decreased Fulton index in hypoxic IL-6 transgenic mice (Figure 8E) and in female (Figures S17F), but not male (Figure S17D), mice exposed to hypoxia+bleomycin. A trend toward lower Fulton index was noted in hypoxic female mice (Figure S15H) treated with rAAV6-BOLA3.

To determine the role of glycine in the actions of BOLA3 in PH, male mice were chronically supplemented with glycine via osmotic pump and in drinking water. Doses were determined empirically to ensure a no more than 1.5-fold chronic increase of glycine in lung tissue in normoxic wildtype mice (Figure S19A). Such supplementation also facilitated persistently elevated glycine levels even when rAAV6-BOLA3 was delivered in hypoxic mice (Figure 8F). Delivery did not affect heart rate, systemic mean arterial pressure, or left ventricular function (Figure S19B–K). Consistent with the predicted pathogenic effects of glycine on the pulmonary vasculature, in normoxic mice, such glycine supplementation, independent of any BOLA3 deficiency (Figure S20A), promoted a modest increase of PCNA (Figure S20B) and vascular remodeling (Figure S20C–D), accompanied by a slight rise in RVSP (Figure S20E) but without alteration of Fulton index (Figure S20F). More importantly, in hypoxic PH mice, glycine supplementation abrogated the protective effect of rAAV6-BOLA3, allowing for persistently elevated PCNA (Figure 8H), pulmonary vascular remodeling, RVSP, and Fulton index (Figure 8I–L), despite forced expression of BOLA3. Taken together, as defined via epistatic gain- and loss-of-function analyses both *in vitro* and *in vivo*, BOLA3 deficiency drives critical endothelial alterations, with a specific dependence on glycine metabolism, in order to promote pulmonary vascular proliferation, remodeling, and hemodynamic manifestations of PH.

Discussion

These findings demonstrate that BOLA3 down-regulation, from epigenetic, hypoxic, or genetic means, promotes pulmonary artery endothelial metabolic re-programming via control of mitochondrial glucose metabolism and glycine homeostasis. *In vivo*, BOLA3 deficiency is both necessary and sufficient to regulate endothelial glycine metabolism and promote PH, relevant to both Group 1 and Group 3 subtypes (Figure 8M). These results

provide a molecular explanation for the enigmatic clinical associations linking PH with hyperglycinemic syndromes and mitochondrial disorders, such as those driven by endogenous BOLA3 mutations. These findings also identify novel metabolic targets, including those involved in epigenetics, iron-sulfur biogenesis, and glycine homeostasis, for diagnostic and therapeutic development.

Our results provide crucial support for the notion of central dysregulation of Fe-S integrity in pulmonary vascular disease, whereby deficiency of BOLA3, a second Fe-S biogenesis protein beyond ISCU½, has now been proven to promote PH. Our data implicate the relevance of BOLA3 to multiple subtypes of PH, including Group 3 PH, a category displaying increasing prevalence and morbidity worldwide without effective treatment options [23]. Our data report substantial consistencies of BOLA3 activity among female and male mice, further emphasizing the broad relevance of this pathobiology. Interestingly, a growing network of genetic, epigenetic (Figure 2), and microRNA-based [4] mechanisms are emerging that control Fe-S biogenesis genes. At the genetic level, future work should more deeply study MMDS2 patients (Figure S6), specifically as to whether BOLA3 mutations that cause MMDS2 [5, 6] or any other linked polymorphisms affecting BOLA3 also carry pathogenic actions in PH, similar to loss-of-function mutations for ISCU½ [4] and the Fe-S biogenesis protein NFU1 [24]. Moreover, it is possible that dysfunctional Fe-S biogenesis may contribute to other clinical syndromes of altered mitochondrial respiration associated with PH [25–28], as well as iron deficiencies known to be important in rodents [29, 30] and humans [31, 32] with PH.

Our findings also contribute to our evolving understanding of altered endothelial metabolism and activation, relevant to PH and other pathophysiologic conditions. Down-regulation of mitochondrial oxidative glucose consumption accompanied by increased glycolytic dependence has been observed in PH diseased PAECs from humans and rodents [33–36]. Our data demonstrate a causal role for BOLA3 deficiency in endothelial repression of respiratory complex function and augmentation of glycolytic flux. Yet, the metabolic shift controlled by BOLA3 increased glycolysis and oxygen consumption (Figure S7A–B), the latter driven by increased FAO and ROS production. Endothelial up-regulation of both glycolysis and oxygen consumption has been described in other contexts where cellular quiescence transitions to an activated state [37]. This observation may seem counter to the original Warburg-like effect in PH [1], but prior studies quantified oxygen consumption primarily in relation to glucose, but not FAO, oxidation. Recent studies have demonstrated that fatty acids control endothelial proliferation via dependence on incorporating FA-derived carbons into nucleotide synthesis [38], particularly under stress [39]. Therefore, our observations expand our understanding of the Warburg-like effect in PH and invoke new questions into the interconnected roles of these processes.

Additionally, the control of glycine metabolism by BOLA3-dependent lipoate synthesis introduces an unexplored mechanism for promoting pulmonary vascular proliferation. Several genetic diseases, driven either by mutations in Fe-S biogenesis components (including the BOLA3-driven MMDS2) or by etiologies independent of Fe-S production, present with metabolic acidosis and hyperglycinemia and are associated with PH [7, 40, 41]. Furthermore, a mutation in the lipoyltransferase gene LIPT1 has been associated with

lipoylation defects and PH [9], offering complementary support to our findings. Also lending credence to our observations, elevated glycine levels have been observed in a hypoxic PH mice [42], individuals non-acclimatized to high altitude and thus at risk for PH [43], and scleroderma patients with PH [44].

Whether other Fe-S biogenesis genes also regulate glycine levels in PH remain unclear, and complex features of this mechanism await interrogation. Prior studies have suggested that glycine may improve systemic hypertension by reducing oxidative stress and increasing nitric oxide [45]; other studies associated higher dietary glycine with more severe hypertension [46]. Glycine may have a protective role against ischemia [47] – an activity evident where hypoxia is known to promote efflux of endogenous glycine, prevent its reuptake [48], and presumably hamper cellular proliferation. In those cases, downregulation of BOLA3 would appear to act as a homeostatic brake to buffer against a substantial loss of net levels of intracellular glycine under hypoxic stress, thus maintaining at least normoxic levels of this amino acid [49]. As such, this may represent a crucial mechanism by which cellular proliferation in hypoxia can be maintained close to normoxic levels – an adaption needed to survive acute hypoxic injury but a detrimental pathophenotype in PAECs and PH during chronic HIF induction. Consequently, we expect that further characterization of the delicate control of glycine homeostasis by BOLA3 and perhaps other Fe-S biogenesis genes will offer substantial insights into the evolution of the proliferation kinetics of PAECs in PH and its subtypes.

In addition to the proliferative response, BOLA3 deficiency led to a state of dysregulated endothelial activation which decreased apoptosis, increased elaboration of vasoconstrictive effectors, and decreased angiogenic potential (Figure 5, S9). While a spatio-temporal model of endothelial pathobiology [50] was proposed for PH, our data predict even greater degree of endothelial complexity than originally anticipated, where, driven by BOLA3 deficiency, pro-proliferative yet dysfunctional angiogenic potential may coalesce in a single, rather than separate, cellular population.

Our findings offer impetus for developing more effective diagnostic and therapeutic targets related to Fe-S biogenesis and glycine metabolism. Utilizing glycine levels as a diagnostic or prognostic biomarker in PH could be possible, singly or in a panel. From a therapeutic perspective, high-throughput drug screening may be effective in identifying small molecules that can directly and effectively controls the levels of Fe-S clusters. Furthermore, altering glycine metabolism or exogenous depletion of glycine could be explored as a therapeutic maneuver. Yet, given the complexity of Fe-S-specific metabolism and glycine in various cell types, maximal efficacy of any targeted drug would necessitate strategy for timing and cell-specific delivery.

Study limitations here exist. *In vitro* and *in vivo*, some responses to BOLA3/GCSH deficiency as well as to glycine were heightened in hypoxia, while normoxic deficiency to BOLA3 (e.g., bleomycin exposure alone in mice) and normoxic glycine supplementation showed less robust phenotypes. As such, hypoxic reprogramming of the endothelial cells appears to provide a permissive state that allows BOLA3 and GCSH downregulation to carry their most robust effects. While the explanation underlying these observations remains

undefined, it is possible that there may be a compensatory molecular response to BOLA3 knockdown in normoxia to prevent as robust of a response as in hypoxia. Furthermore, it is notable that some, but not all, *in vivo* models of PH studied displayed an alteration of RV remodeling dependent upon siRNA or rAAV6-BOLA3 delivery. While varying hemodynamic severity across PH models may have contributed, confounding delivery of BOLA3 reagents to the RV cardiomyocytes and alteration of CPT1A and FAO (Figure S13) may have partially compromised the effect of pulmonary vascular improvements on the RV. Such a notion more broadly sets the stage for studies to determine the exact cell-specific actions of BOLA3 in vascular and non-vascular (RV) cell types driving PH.

In summary, these findings define a paradigm whereby BOLA3 acts as a crucial lynchpin connecting Fe-S-dependent oxidative respiration and glycine homeostasis with endothelial metabolic re-programming critical to PH pathogenesis. These results alter our fundamental understanding of endothelial dysfunction in PH, offer a molecular explanation underlying the associations linking hyperglycinemia and mitochondrial disorders with PH, and present novel metabolic pathways for diagnostic and therapeutic development.

Supplementary Material

Refer to Web version on PubMed Central for supplementary material.

Acknowledgments

We thank W. Kim (University of North Carolina, Chapel Hill) for the constitutively active HIF-2α plasmid.

The authors would like to acknowledge The Center for Organ Recovery & Education (CORE) as well as organ donors and their families for the generous donation of tissues used in this study.

Sources of Funding

This work was supported by NIH grants R01 HL124021, HL 122596, HL 138437, and UH2 TR002073 as well as the American Heart Association Established Investigator Award 18EIA33900027 (S.Y.C.).

References

1. Chan SY and Rubin LJ. Metabolic dysfunction in pulmonary hypertension: From basic science to clinical practice Eur Respir Rev. 2017; 26:170094. [PubMed: 29263174]
2. Chan SY, Zhang YY, Hemann C, Mahoney CE, Zweier JL and Loscalzo J. MicroRNA-210 controls mitochondrial metabolism during hypoxia by repressing the iron-sulfur cluster assembly proteins ISCU½. Cell Metab. 2009; 10:273–284. [PubMed: 19808020]
3. Rouault TA. Biogenesis of iron-sulfur clusters in mammalian cells: new insights and relevance to human disease. Dis Model Mech. 2012; 5:155–164. [PubMed: 22382365]
4. White K, Lu Y, Annis S, Hale AE, Chau BN, Dahlman JE, Hemann C, Opotowsky AR, Vargas SO, Rosas I, Perrella MA, Osorio JC, Haley KJ, Graham BB, Kumar R, Saggar R, Saggar R, Wallace WD, Ross DJ, Khan OF, Bader A, Gochuico BR, Matar M, Polach K, Johannessen NM, Prosser HM, Anderson DG, Langer R, Zweier JL, Bindoff LA, Systrom D, Waxman AB, Jin RC and Chan SY. Genetic and hypoxic alterations of the microRNA-210-ISCU½ axis promote iron-sulfur deficiency and pulmonary hypertension. EMBO Mol Med. 2015; 7:695–713. [PubMed: 25825391]
5. Cameron JM, Janer A, Levandovskiy V, Mackay N, Rouault TA, Tong WH, Ogilvie I, Shoubridge EA and Robinson BH. Mutations in iron-sulfur cluster scaffold genes NFU1 and BOLA3 cause a fatal deficiency of multiple respiratory chain and 2-oxoacid dehydrogenase enzymes. Am J Hum Genet. 2011; 89:486–495. [PubMed: 21944046]

6. Haack TB, Rolinski B, Haberberger B, Zimmermann F, Schum J, Strecker V, Graf E, Athing U, Hoppen T, Wittig I, Sperl W, Freisinger P, Mayr JA, Strom TM, Meitinger T and Prokisch H. Homozygous missense mutation in BOLA3 causes multiple mitochondrial dysfunctions syndrome in two siblings. J Inherit Metab Dis. 2013; 36:55–62. [PubMed: 22562699]

7. Navarro-Sastre A, Tort F, Stehling O, Uzarska MA, Arranz JA, Del Toro M, Labayru MT, Landa J, Font A, Garcia-Villoria J, Merinero B, Ugarte M, Gutierrez-Solana LG, Campistol J, Garcia-Cazorla A, Vaquerizo J, Riudor E, Briones P, Elpeleg O, Ribes A and Lill R. A fatal mitochondrial disease is associated with defective NFU1 function in the maturation of a subset of mitochondrial Fe-S proteins. Am J Hum Genet. 2011; 89:656–667. [PubMed: 22077971]

8. Ahting U, Mayr JA, Vanlander AV, Hardy SA, Santra S, Makowski C, Alston CL, Zimmermann FA, Abela L, Plecko B, Rohrbach M, Spranger S, Seneca S, Rolinski B, Hagendorff A, Hempel M, Sperl W, Meitinger T, Smet J, Taylor RW, Van Coster R, Freisinger P, Prokisch H and Haack TB. Clinical, biochemical, and genetic spectrum of seven patients with NFU1 deficiency. Front Genet. 2015; 6:123. [PubMed: 25918518]

9. Tort F, Ferrer-Cortes X, Thio M, Navarro-Sastre A, Matalonga L, Quintana E, Bujan N, Arias A, Garcia-Villoria J, Acquaviva C, Vianey-Saban C, Artuch R, Garcia-Cazorla A, Briones P and Ribes A. Mutations in the lipoyltransferase LIPT1 gene cause a fatal disease associated with a specific lipoylation defect of the 2-ketoacid dehydrogenase complexes. Hum Mol Genet. 2014; 23:1907–1915. [PubMed: 24256811]

10. Uzarska MA, Nasta V, Weiler BD, Spantgar F, Ciofi-Baffoni S, Saviello MR, Gonnelli L, Muhlenhoff U, Banci L and Lill R. Mitochondrial Bol1 and Bol3 function as assembly factors for specific iron-sulfur proteins. Elife. 2016; 5:e16673. [PubMed: 27532772]

11. Hiltunen JK, Autio KJ, Schonauer MS, Kursu VA, Dieckmann CL and Kastaniotis AJ. Mitochondrial fatty acid synthesis and respiration. Biochim Biophys Acta. 2010;1797:1195–202. [PubMed: 20226757]

12. Mayr JA, Feichtinger RG, Tort F, Ribes A and Sperl W. Lipoic acid biosynthesis defects. J Inherit Metab Dis. 2014; 37:553–563. [PubMed: 24777537]

13. Jain M, Nilsson R, Sharma S, Madhusudhan N, Kitami T, Souza AL, Kafri R, Kirschner MW, Clish CB and Mootha VK. Metabolite profiling identifies a key role for glycine in rapid cancer cell proliferation. Science. 2012; 336:1040–1044. [PubMed: 22628656]

14. Bertero T, Lu Y, Annis S, Hale A, Bhat B, Saggar R, Saggar R, Wallace WD, Ross DJ, Vargas SO, Graham BB, Kumar R, Black SM, Fratz S, Fineman JR, West JD, Haley KJ, Waxman AB, Chau BN, Cottrill KA and Chan SY. Systems-level regulation of microRNA networks by miR-130/301 promotes pulmonary hypertension. J Clin Invest. 2014; 124:3514–3528. [PubMed: 24960162]

15. Steiner MK, Syrkina OL, Kolliputi N, Mark EJ, Hales CA and Waxman AB. Interleukin-6 overexpression induces pulmonary hypertension. Circ Res. 2009; 104:236–244. [PubMed: 19074475]

16. Gille T, Didier M, Rotenberg C, Delbrel E, Marchant D, Sutton A, Dard N, Haine L, Voituron N, Bernaudin JF, Valeyre D, Nunes H, Besnard V, Boncoeur E and Planes C. Intermittent Hypoxia Increases the Severity of Bleomycin-Induced Lung Injury in Mice. Oxid Med Cell Longev. 2018; 2018:1240192. [PubMed: 29725493]

17. Michelakis ED, Gurtu V, Webster L, Barnes G, Watson G, Howard L, Cupitt J, Paterson I, Thompson RB, Chow K, O'Regan DP, Zhao L, Wharton J, Kiely DG, Kinnaird A, Boukouris AE, White C, Nagendran J, Freed DH, Wort SJ, Gibbs JSR and Wilkins MR. Inhibition of pyruvate dehydrogenase kinase improves pulmonary arterial hypertension in genetically susceptible patients. Sci Transl Med. 2017; 9:eaao4583. [PubMed: 29070699]

18. Tuganova A, Boulatnikov I and Popov KM. Interaction between the individual isoenzymes of pyruvate dehydrogenase kinase and the inner lipoyl-bearing domain of transacetylase component of pyruvate dehydrogenase complex. Biochem J. 2002; 366:129–136. [PubMed: 11978179]

19. Lodi A, Tiziani S, Khanim FL, Drayson MT, Gunther UL, Bunce CM and Viant MR. Hypoxia triggers major metabolic changes in AML cells without altering indomethacin-induced TCA cycle deregulation. ACS Chem Biol. 2011; 6:169–175. [PubMed: 20886892]

20. Kim D, Fiske BP, Birsoy K, Freinkman E, Kami K, Possemato RL, Chudnovsky Y, Pacold ME, Chen WW, Cantor JR, Shelton LM, Gui DY, Kwon M, Ramkissoon SH, Ligon KL, Kang SW,

Snuderl M, Vander Heiden MG and Sabatini DM. SHMT2 drives glioma cell survival in ischaemia but imposes a dependence on glycine clearance. Nature. 2015; 520:363–367. [PubMed: 25855294]

21. Dahlman JE, Barnes C, Khan OF, Thiriot A, Jhunjunwala S, Shaw TE, Xing Y, Sager HB, Sahay G, Speciner L, Bader A, Bogorad RL, Yin H, Racie T, Dong Y, Jiang S, Seedorf D, Dave A, Singh Sandhu K, Webber MJ, Novobrantseva T, Ruda VM, Lytton-Jean AK, Levins CG, Kalish B, Mudge DK, Perez M, Abezgauz L, Dutta P, Smith L, Charisse K, Kieran MW, Fitzgerald K, Nahrendorf M, Danino D, Tuder RM, von Andrian UH, Akinc A, Panigrahy D, Schroeder A, Koteliansky V, Langer R and Anderson DG. In vivo endothelial siRNA delivery using polymeric nanoparticles with low molecular weight. Nat Nanotechnol. 2014; 9:648–655. [PubMed: 24813696]
22. Ellis BL, Hirsch ML, Barker JC, Connelly JP, Steininger RJ 3rd and Porteus MH. A survey of ex vivo/in vitro transduction efficiency of mammalian primary cells and cell lines with Nine natural adeno-associated virus (AAV1–9) and one engineered adeno-associated virus serotype. Virol J. 2013; 10:74. [PubMed: 23497173]
23. Seeger W, Adir Y, Barbera JA, Champion H, Coghlan JG, Cottin V, De Marco T, Galie N, Ghio S, Gibbs S, Martinez FJ, Semigran MJ, Simonneau G, Wells AU and Vachiery JL. Pulmonary hypertension in chronic lung diseases. J Am Coll Cardiol. 2013; 62:D109–116. [PubMed: 24355635]
24. Barclay AR, Sholler G, Christodolou J, Shun A, Arbuckle S, Dorney S and Stormon MO. Pulmonary hypertension--a new manifestation of mitochondrial disease. J Inherit Metab Dis. 2005; 28:1081–1089. [PubMed: 16435201]
25. Sproule DM, Dyme J, Coku J, de Vinck D, Rosenzweig E, Chung WK and De Vivo DC. Pulmonary artery hypertension in a child with MELAS due to a point mutation of the mitochondrial tRNA((Leu)) gene (m.3243A > G). J Inherit Metab Dis. 2008; 31:497–503. [PubMed: 18181029]
26. Hung PC, Wang HS, Chung HT, Hwang MS and Ro LS. Pulmonary hypertension in a child with mitochondrial A3243G point mutation. Brain Dev. 2012; 34:866–868. [PubMed: 22455997]
27. Rivera H, Martin-Hernandez E, Delmiro A, Garcia-Silva MT, Quijada-Fraile P, Muley R, Arenas J, Martin MA and Martinez-Azorin F. A new mutation in the gene encoding mitochondrial seryl-tRNA synthetase as a cause of HUPRA syndrome. BMC Nephrol. 2013; 14:195. [PubMed: 24034276]
28. Catteruccia M, Verrigni D, Martinelli D, Torraco A, Agovino T, Bonafe L, D'Amico A, Donati MA, Adorisio R, Santorelli FM, Carrozzo R, Bertini E and Dionisi-Vici C. Persistent pulmonary arterial hypertension in the newborn (PPHN): a frequent manifestation of TMEM70 defective patients. Mol Genet Metab. 2014; 111:353–359. [PubMed: 24485043]
29. Ghosh MC, Zhang DL, Jeong SY, Kovtunovych G, Ollivierre-Wilson H, Noguchi A, Tu T, Senecal T, Robinson G, Crooks DR, Tong WH, Ramaswamy K, Singh A, Graham BB, Tuder RM, Yu ZX, Eckhaus M, Lee J, Springer DA and Rouault TA. Deletion of iron regulatory protein 1 causes polycythemia and pulmonary hypertension in mice through translational derepression of HIF2alpha. Cell Metab. 2013; 17:271–281. [PubMed: 23395173]
30. Cotroneo E, Ashek A, Wang L, Wharton J, Dubois O, Bozorgi S, Busbridge M, Alavian KN, Wilkins MR and Zhao L. Iron homeostasis and pulmonary hypertension: iron deficiency leads to pulmonary vascular remodeling in the rat. Circ Res. 2015; 116:1680–1690. [PubMed: 25767292]
31. Ruiter G, Lankhorst S, Boonstra A, Postmus PE, Zweegman S, Westerhof N, van der Laarse WJ and Vonk-Noordegraaf A. Iron deficiency is common in idiopathic pulmonary arterial hypertension. Eur Respir J. 2011; 37:1386–1391. [PubMed: 20884742]
32. Rhodes CJ, Howard LS, Busbridge M, Ashby D, Kondili E, Gibbs JS, Wharton J and Wilkins MR. Iron deficiency and raised hepcidin in idiopathic pulmonary arterial hypertension: clinical prevalence, outcomes, and mechanistic insights. J Am Coll Cardiol. 2011; 58:300–309. [PubMed: 21737024]
33. Xu W, Koeck T, Lara AR, Neumann D, DiFilippo FP, Koo M, Janocha AJ, Masri FA, Arroliga AC, Jennings C, Dweik RA, Tuder RM, Stuehr DJ and Erzurum SC. Alterations of cellular bioenergetics in pulmonary artery endothelial cells. Proc Natl Acad Sci U S A. 2007; 104:1342–1347. [PubMed: 17227868]

34. Diebold I, Hennigs JK, Miyagawa K, Li CG, Nickel NP, Kaschwich M, Cao A, Wang L, Reddy S, Chen PI, Nakahira K, Alcazar MA, Hopper RK, Ji L, Feldman BJ and Rabinovitch M. BMPR2 preserves mitochondrial function and DNA during reoxygenation to promote endothelial cell survival and reverse pulmonary hypertension. Cell Metab. 2015; 21:596–608. [PubMed: 25863249]
35. Sun X, Sharma S, Fratz S, Kumar S, Rafikov R, Aggarwal S, Rafikova O, Lu Q, Burns T, Dasarathy S, Wright J, Schreiber C, Radman M, Fineman JR and Black SM. Disruption of endothelial cell mitochondrial bioenergetics in lambs with increased pulmonary blood flow. Antioxid Redox Signal. 2013; 18:1739–1752. [PubMed: 23244702]
36. Sun X, Kumar S, Sharma S, Aggarwal S, Lu Q, Gross C, Rafikova O, Lee SG, Dasarathy S, Hou Y, Meadows ML, Han W, Su Y, Fineman JR and Black SM. Endothelin-1 induces a glycolytic switch in pulmonary arterial endothelial cells via the mitochondrial translocation of endothelial nitric oxide synthase. Am J Respir Cell Mol Biol. 2014; 50:1084–1095. [PubMed: 24392990]
37. Wilhelm K, Happel K, Eelen G, Schoors S, Oellerich MF, Lim R, Zimmermann B, Aspalter IM, Franco CA, Boettger T, Braun T, Fruttiger M, Rajewsky K, Keller C, Bruning JC, Gerhardt H, Carmeliet P and Potente M. FOXO1 couples metabolic activity and growth state in the vascular endothelium. Nature. 2016; 529:216–220. [PubMed: 26735015]
38. Schoors S, Bruning U, Missiaen R, Queiroz KC, Borgers G, Elia I, Zecchin A, Cantelmo AR, Christen S, Goveia J, Heggermont W, Godde L, Vinckier S, Van Veldhoven PP, Eelen G, Schoonjans L, Gerhardt H, Dewerchin M, Baes M, De Bock K, Ghesquiere B, Lunt SY, Fendt SM and Carmeliet P. Fatty acid carbon is essential for dNTP synthesis in endothelial cells. Nature. 2015; 520:192–197. [PubMed: 25830893]
39. Wong BW, Wang X, Zecchin A, Thienpont B, Cornelissen I, Kalucka J, Garcia-Caballero M, Missiaen R, Huang H, Bruning U, Blacher S, Vinckier S, Goveia J, Knobloch M, Zhao H, Dierkes C, Shi C, Hagerling R, Moral-Darde V, Wyns S, Lippens M, Jessberger S, Fendt SM, Luttun A, Noel A, Kiefer F, Ghesquiere B, Moons L, Schoonjans L, Dewerchin M, Eelen G, Lambrechts D and Carmeliet P. The role of fatty acid beta-oxidation in lymphangiogenesis. Nature. 2017; 542:49–54. [PubMed: 28024299]
40. del Toro M, Arranz JA, Macaya A, Riudor E, Raspall M, Moreno A, Vazquez E, Ortega A, Matsubara Y, Kure S and Roig M. Progressive vacuolating glycine leukoencephalopathy with pulmonary hypertension. Ann Neurol. 2006; 60:148–152. [PubMed: 16802295]
41. Cataltepe S, van Marter LJ, Kozakewich H, Wessel DL, Lee PJ and Levy HL. Pulmonary hypertension associated with nonketotic hyperglycinaemia. J Inherit Metab Dis. 2000; 23:137–144. [PubMed: 10801055]
42. Izquierdo-Garcia JL, Arias T, Rojas Y, Garcia-Ruiz V, Santos A, Martin-Puig S and Ruiz-Cabello J. Metabolic Reprogramming in the Heart and Lung in a Murine Model of Pulmonary Arterial Hypertension. Front Cardiovasc Med. 2018; 5:110. [PubMed: 30159317]
43. Luo Y, Zhu J and Gao Y. Metabolomic analysis of the plasma of patients with high-altitude pulmonary edema (HAPE) using 1H NMR. Mol Biosyst. 2012; 8:1783–1788. [PubMed: 22498880]
44. Deidda M, Piras C, Cadeddu Dessalvi C, Locci E, Barberini L, Orofino S, Musu M, Mura MN, Manconi PE, Finco G, Atzori L and Mercuro G. Distinctive metabolomic fingerprint in scleroderma patients with pulmonary arterial hypertension. Int J Cardiol. 2017; 241:401–406. [PubMed: 28476520]
45. El Hafidi M, Perez I and Banos G. Is glycine effective against elevated blood pressure? Curr Opin Clin Nutr Metab Care. 2006; 9:26–31. [PubMed: 16444815]
46. Stamler J, Brown IJ, Daviglus ML, Chan Q, Miura K, Okuda N, Ueshima H, Zhao L and Elliott P. Dietary glycine and blood pressure: the International Study on Macro/Micronutrients and Blood Pressure. Am J Clin Nutr. 2013; 98:136–145. [PubMed: 23656904]
47. Wang W, Wu Z, Dai Z, Yang Y, Wang J and Wu G. Glycine metabolism in animals and humans: implications for nutrition and health. Amino Acids. 2013; 45:463–477. [PubMed: 23615880]
48. Bhat GB, Tinsley SB, Tolson JK, Patel JM and Block ER. Hypoxia increases the susceptibility of pulmonary artery endothelial cells to hydrogen peroxide injury. J Cell Physiol. 1992; 151:228–238. [PubMed: 1572899]

49. Oldham WM, Clish CB, Yang Y and Loscalzo J. Hypoxia-Mediated Increases in L-2-hydroxyglutarate Coordinate the Metabolic Response to Reductive Stress. Cell Metab. 2015; 22:291–303. [PubMed: 26212716]

50. Michelakis ED. Spatio-temporal diversity of apoptosis within the vascular wall in pulmonary arterial hypertension: heterogeneous BMP signaling may have therapeutic implications. Circ Res. 2006; 98:172–175. [PubMed: 16456109]

Clinical Perspective

What is new?

- We demonstrate that epigenetic and hypoxic repression of the iron-sulfur biogenesis protein BOLA3 promotes pulmonary artery endothelial metabolic re-programming and dysfunction.
- To do so, BOLA3 deficiency induces alterations of mitochondrial electron transport, glycolysis, and fatty acid oxidation.
- BOLA3 deficiency also represses lipoate biosynthesis, thus inhibiting the glycine cleavage system, increasing glycine accumulation, and promoting endothelial proliferation.
- *In vivo*, we find that BOLA3 deficiency is both necessary and sufficient to regulate endothelial glycine metabolism and to promote hemodynamic and histologic manifestations of pulmonary hypertension.

What are the clinical implications?

- These findings define BOLA3 as a crucial lynchpin connecting oxidative metabolism and glycine homeostasis with endothelial dysfunction in pulmonary hypertension.
- These results provide a molecular explanation for the enigmatic clinical associations linking pulmonary hypertension with hyperglycinemic syndromes and mitochondrial disorders, such as those driven by endogenous BOLA3 mutations.
- These findings also identify novel metabolic targets, including those involved in epigenetics, iron-sulfur biogenesis, and glycine homeostasis, for diagnostic and therapeutic development in this devastating disease.

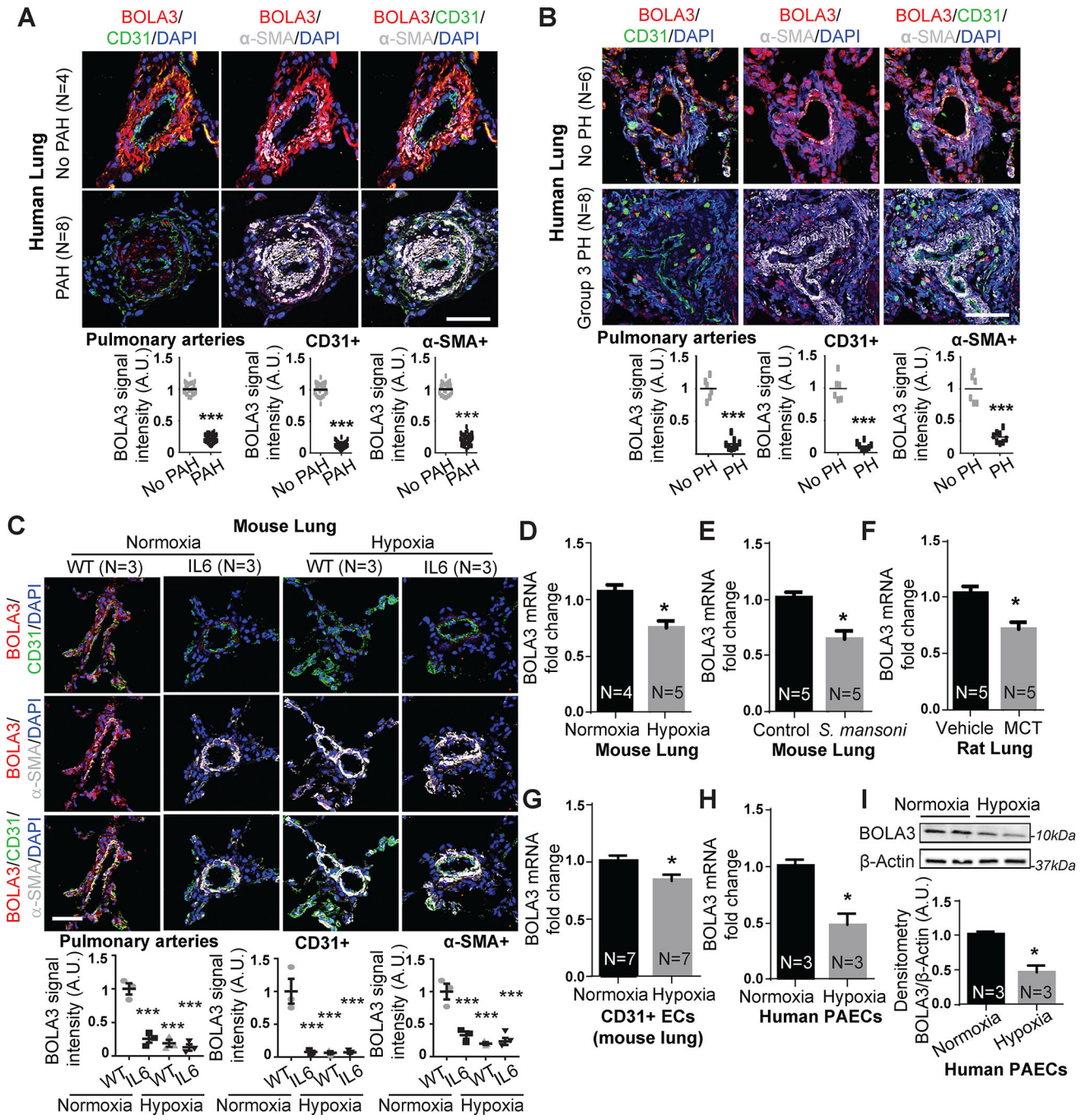

Figure 1: Down-regulation of BOLA3 across multiple *in vitro* and *in vivo* models of PH.

(A-C) Fluorescence microscopy of human lung from Group 1 PAH **(A)** and Group 3 PH **(B)** vs. non-PH patients; interleukin-6 (IL-6) transgenic mice (without or without hypoxia); and hypoxic wildtype (WT) mice **(C)** revealed reduced BOLA3 expression in endothelium (CD31 label) and smooth muscle (α-SMA label). Scale bar: 50μm. **(D-G)** By RT-qPCR, BOLA3 transcript expression was decreased in lung from hypoxic PH mice (10% O2) **(D)**, PH mice infected with *S. mansoni* **(E)**, and monocrotaline (MCT)-exposed PH rats **(F)**. **(G)** Similarly, BOLA3 transcript expression was decreased in CD31-positive pulmonary

endothelial cells (ECs) isolated from chronically hypoxic PH mice. **(H-I)** By RT-qPCR and immunoblotting respectively, BOLA3 was decreased at the transcript **(H)** and protein **(I)** levels in cultured hypoxic human pulmonary arterial endothelial cells (PAECs). In **(I)**, representative immunoblot is shown with densitometry calculated across 3 separate replicates. In all panels, mean expression in controls (no PAH, no PH, WT, vehicle, control, normoxia) was normalized to a fold change of 1, to which relevant samples were compared (N = 3–8/group). Data represent the mean ± SEM (*P < 0.05, ***P < 0.001).

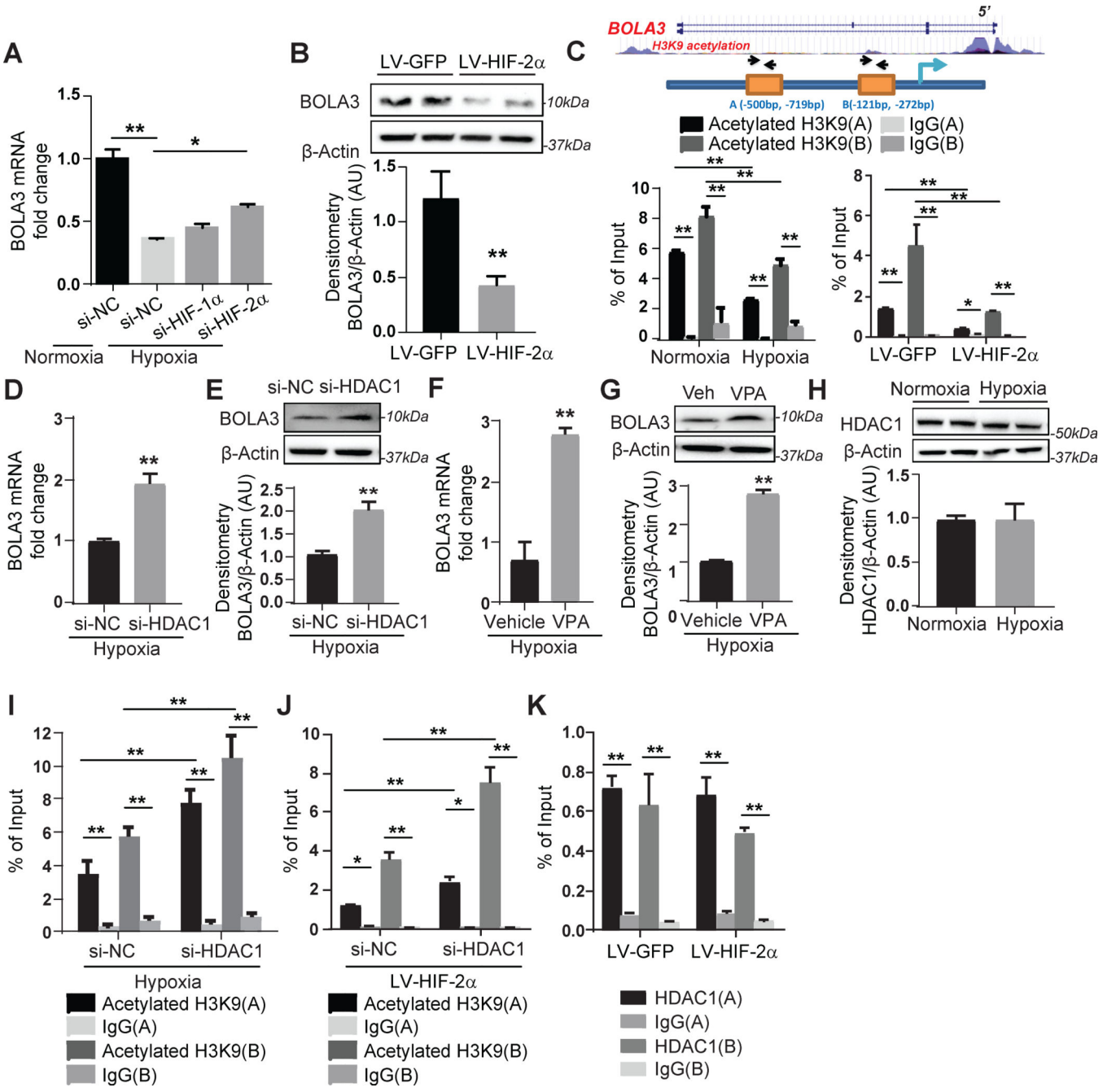

Figure 2: Hypoxia mediates transcriptional repression of BOLA3 via HIF-2α/HDAC/histone acetylation pathway.

(A) Transfection of siRNA targeting hypoxia induced factor (HIF)-2α, but not HIF-1α, partially rescued BOLA3 expression in hypoxic human PAECs. **(B)** Lentivirus (LV)-mediated forced expression of a constitutively active HIF-2α in PAECs inhibited BOLA3. **(C)** ChIP-qPCR via immunoprecipitation of acetylated histone 3 lysine 9 (H3K9) and PCR detection of BOLA3 promoter sites indicated acetylated H3K9 enrichment of the BOLA3 promoter (sites A, B), which was decreased by hypoxia (left) or constitutive HIF-2α (right). **(D-G)** siRNA knockdown of histone deacetylase 1 (HDAC1) as well as valproic acid (VPA,

3mM), a HDAC inhibitor, both rescued BOLA3 transcript and protein expression in hypoxic PAECs. **(H)** Expression of HDAC1 remained unchanged in hypoxic PAECs. **(I-J)** siRNA knockdown of HDAC1 enhanced enrichment of H3K9 acetylation at the BOLA3 promotor in hypoxia (**I**) or with constitutive HIF-2α expression **(J). (K)** ChIP-qPCR via immunoprecipitation of HDAC1 indicated HDAC1 enrichment at BOLA3 promoter sites that was not altered with constitutive HIF-2α expression. In all panels measuring fold change, mean expression in control groups (si-NC, LV-GFP, normoxia, vehicle) was normalized to fold change of 1, to which relevant samples were compared (N = 3/group). Data represent the mean ± SEM (*P < 0.05, **P < 0.01).

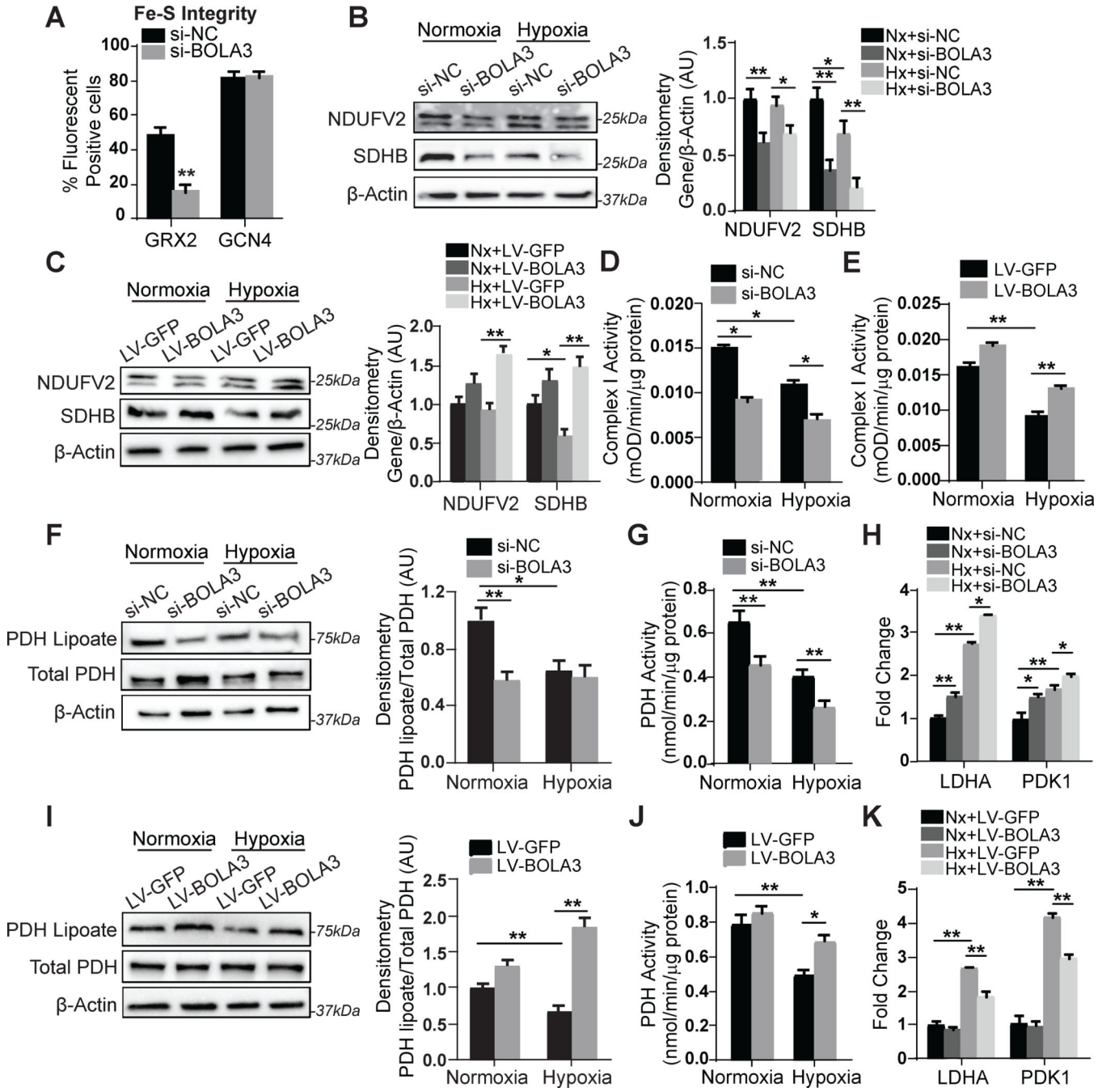

Figure 3: BOLA3 controls Fe-S integrity and mitochondrial complex activity as well as mitochondrial lipoate-containing 2-oxoacid dehydrogenases.

(A) Knockdown of BOLA3 to PAECs compromised Fe-S integrity, as assessed by lentiviral delivery of Fe-S-dependent (glutaredoxin 2, GRX2) vs. Fe-S-independent (GCN4) fluorescent sensors. **(B)** By immunoblot and densitometry, expression of NDUFV2 (doublet band) and SDHB, representative mitochondrial Complex I and II components respectively, was decreased by BOLA3 knockdown in normoxia (Nx) and hypoxia (Hx); however, hypoxia alone did not robustly alter their expression. **(C)** Conversely, forced lentiviral expression of BOLA3 compared with GFP control increased NDUFV2 and SDHB

expression in normoxia and hypoxia. **(D-E)** In PAECs, hypoxia-dependent Fe-S-dependent Complex I activity was down-regulated by BOLA3 knockdown **(D)** and conversely rescued by forced BOLA3 expression **(E)**. **(F)** PAEC expression of lipoate-containing pyruvate dehydrogenase (PDH) was decreased by BOLA3 knockdown in normoxia and was phenocopied by hypoxic exposure. (**G**) In correlation, PDH activity was decreased by BOLA3 knockdown in normoxia and by hypoxic exposure; BOLA3 knockdown in combination with hypoxia further decreased PDH activity. **(H)** In the setting of increased lactate dehydrogenase (LDHA) and pyruvate dehydrogenase kinase 1 (PDK1) expression in hypoxia, by RT-qPCR, BOLA3 knockdown in PAECs increased LDHA and PDK1 in normoxia and hypoxia. **(I-J)** Conversely, BOLA3 overexpression increased lipoate-containing PDH **(I)** and increased PDH activity in normoxia and hypoxia **(J)**. **(K)** BOLA3 overexpression blunted the upregulation of LDHA and PDK1 specifically in hypoxia. In all panels, mean expression of control groups (si-NC, Nx+si-NC, Nx+LV-GFP) was normalized to fold change of 1, to which all relevant samples were compared (N = 3/group). Data represent the mean ± SEM (*P < 0.05, **P < 0.01).

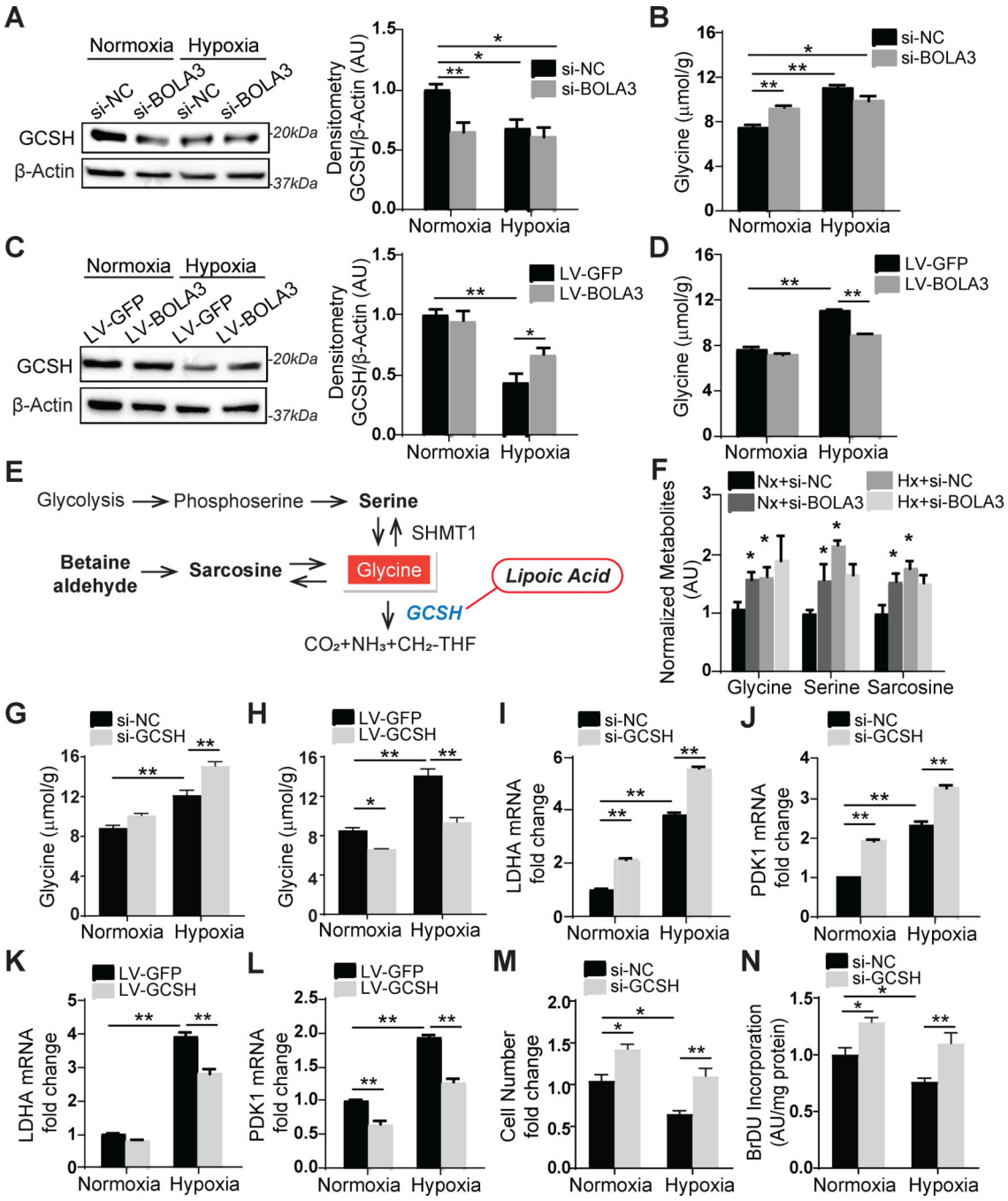

Figure 4. BOLA3 deficiency modulates glycine metabolism by inhibiting GCSH in PAECs.

(A) Via immunoblot and densitometry, in PAECs, BOLA3 knockdown inhibited glycine cleavage system H protein (GCSH) in normoxia, thus phenocopying hypoxia alone. **(B)** BOLA3 knockdown in normoxia promoted intracellular glycine accumulation, again similar to hypoxia. **(C-D)** Conversely, in hypoxia, forced BOLA3 expression reversed the reduction of GCSH **(C)** and blunted consequent glycine accumulation **(D)**. **(E-F)** By mass spectrometry, BOLA3 knockdown in normoxia (Nx) phenocopied hypoxia (Hx) by increasing accumulation of glycine as well as its relevant metabolites, serine and sarcosine

(F), as predicted by known metabolic schema **(E)**. **(G-H)** GCSH knockdown augmented glycine accumulation particularly in hypoxia, while forced expression of GCSH reversed the accumulation of glycine in hypoxia. **(I-L)** GCSH knockdown further enhanced LDHA **(I)** and PDK1 **(J)** expression in hypoxia, which was reversed by GCSH overexpression **(K, L)**. **(M-N)** GCSH knockdown increased PAECs proliferation, as measured by cell number count **(M)** and BrdU incorporation **(N)**. In all panels, mean expression of control groups (Nx si-NC, Nx LV-GFP) was normalized to fold change of 1, to which relevant samples were compared (N = 3/group). Data represent the mean ± SEM (*P < 0.05, **P < 0.01).

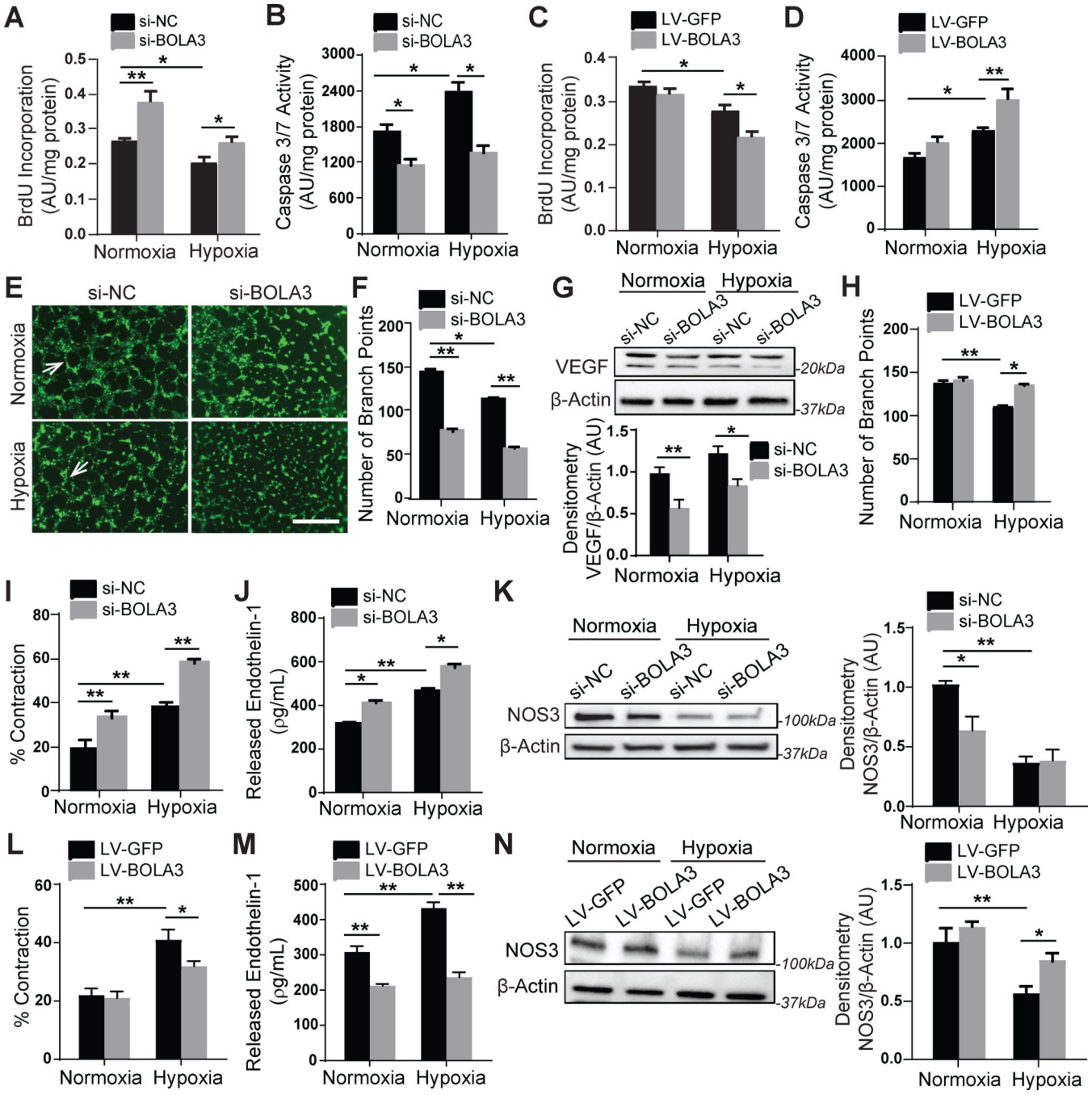

Figure 5: BOLA3 deficiency increases proliferation, inhibits apoptosis and angiogenesis, and promotes vasoconstriction in PAECs.

(A-B) As reflected by BrdU incorporation and apoptotic caspase 3/7 activation, BOLA3 knockdown increased PAEC proliferation and reduced apoptosis in both normoxia and hypoxia. **(C-D)** Conversely, forced BOLA3 expression inhibited proliferation and promoted apoptotic signaling in hypoxia. **(E-F)** BOLA3 knockdown inhibited *in vitro* angiogenic potential, as measured by tube formation in matrix gel in normoxia and hypoxia **(E)**, white arrows indicate representative full tubes and branch point quantification **(F)**. Scale bar,

200μm. **(G)** BOLA3 knockdown down-regulated vascular endothelial growth factor (VEGF) as assessed by immunoblot. **(H)** Conversely, forced BOLA3 expression increased *in vitro* tube formation in hypoxic PAECs. **(I)** As quantified by a gel matrix contraction assay encompassing the exposure of PASMCs in gel matrix to conditioned serum-free medium from PAECs, knockdown of BOLA3 in PAECs produced conditioned media that increased PASMC contraction in normoxia and hypoxia. **(J)** As quantified by ELISA, BOLA3 knockdown increased secreted endothelin-1 (ET-1) production in normoxia and hypoxia. **(K)** As assessed by immunoblot and densitometry, BOLA3 knockdown in normoxia inhibited nitric oxide synthase 3 (NOS3) expression, at least partially phenocopying the more robust downregulation in hypoxia. **(L)** Conditioned serum-free medium from PAECs constitutively expressing BOLA3 transgene blunted the hypoxic induction of PASMC contraction in matrix gel. **(M)** Forced BOLA3 expression inhibited ET-1 release in normoxia and hypoxia. **(N)** More evident in hypoxia, constitutive BOLA3 transgene expression rescued NOS3 expression. In panels G, K, and N, mean expression of control group (Nx si-NC or Nx LV-GFP) was normalized to fold change of 1, to which relevant samples were compared. For all panels, N = 3–6 replicates/group. Data represent the mean ± SEM (*P < 0.05, **P < 0.01).

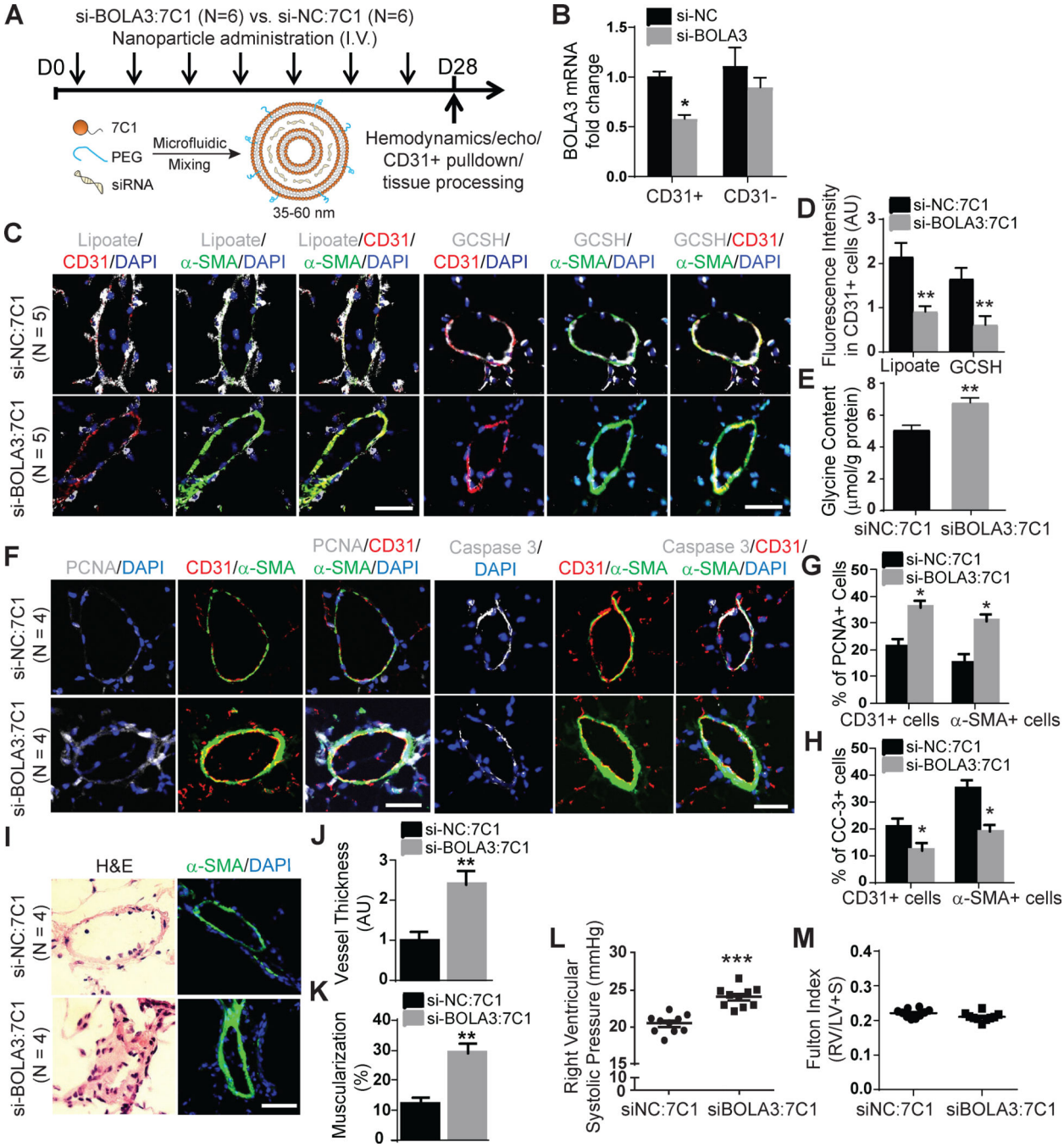

Figure 6: Endothelial-specific delivery of BOLA3 siRNA dysregulates lipoate synthesis and glycine metabolism, thus promoting PH.

(A) Wildtype C57Bl6 mice received intravenous injections of either si-BOLA3:7C1 or si-NC:7C1 nanoparticles every 4 days for 28 days to target vascular endothelium of mice. **(B)** Pulmonary vascular delivery of si-BOLA3: 7C1 nanoparticles reduced BOLA3 RNA expression in isolated CD31+ pulmonary endothelial cells, but not in CD31- pulmonary cells (N = 4/group). **(C-E)** 7C1:si-BOLA3 reduced lipoate (white, left 3 columns) and GCSH (white, right 3 columns) expression by *in situ* fluorescence microscopy and increased

glycine content by fluorometric assay in mouse lung tissues. **(F-H)** 7C1:si-BOLA3 increased the proliferation marker PCNA but inhibited the apoptotic marker cleaved caspase 3 (CC-3) in both CD31+ endothelial and α-SMA+ cells in mouse vasculature. **(I-K)** si-BOLA3:7C1 increased pulmonary vessel thickness **(J)** and muscularization **(K)** as assessed by hematoxylin and eosin staining (left column, **I**) as well as α-SMA staining (green, right column, **I**). **(L-M)** 7C1:si-BOLA3 elevated right ventricular systolic pressure measured by right heart catheterization but did not affect right ventricular hypertrophy (Fulton index, RV/LV+S), N = 10 mice/group. In panel B, mean expression of control group (si-NC) was normalized to fold change of 1, to which relevant samples were compared. Data represent the mean ± SEM. (*P < 0.05, **P < 0.01, ***P<0.001). Scale bars, 50μm.

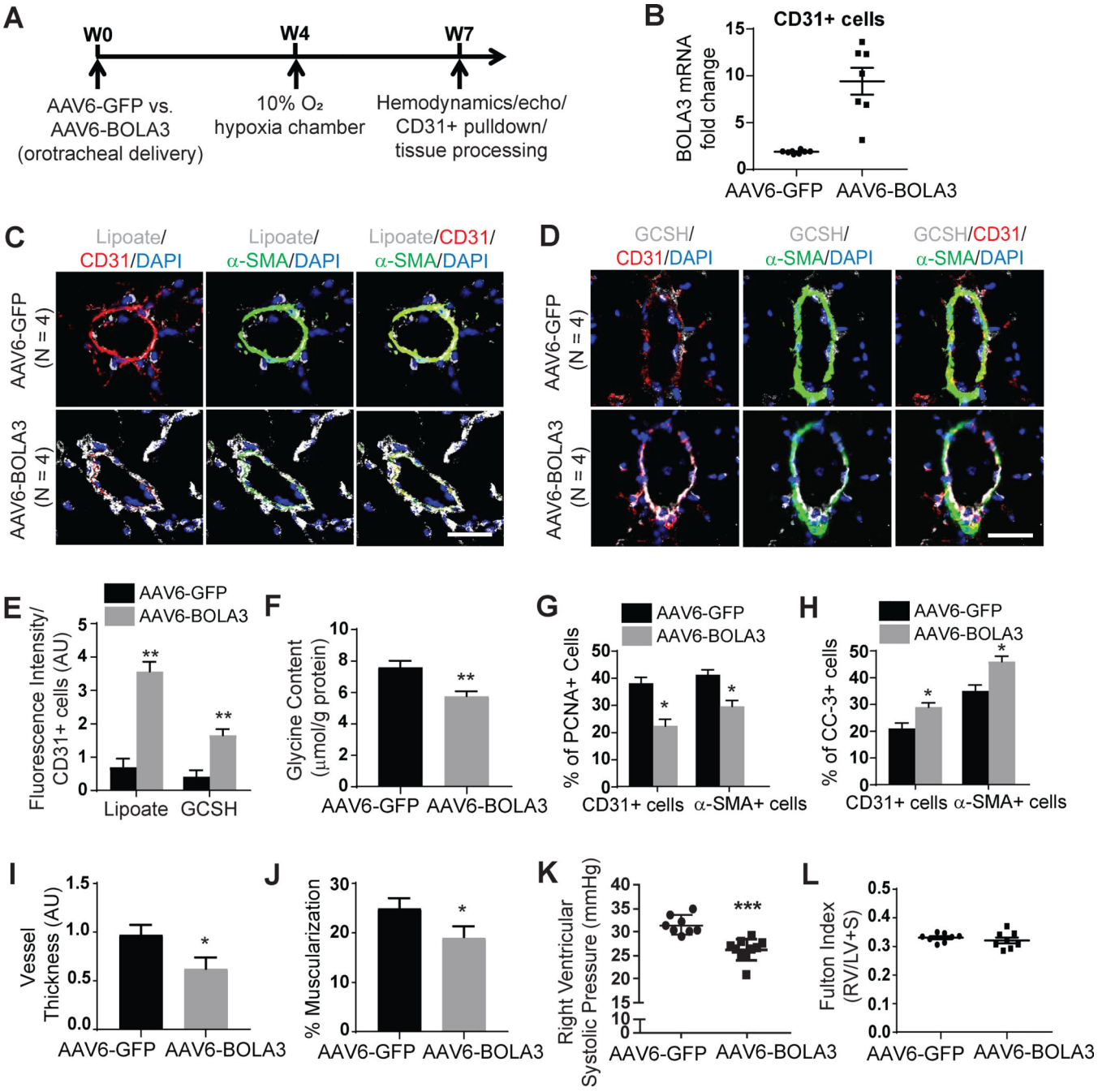

Figure 7: Forced expression of pulmonary vascular BOLA3 prevents PH in mice.

(A) As diagrammed, either AAV6-GFP or AAV6- BOLA3 was administered to wildtype C57Bl6 mice via an orotracheal route 4 weeks prior to hypoxic exposure for 3 weeks. **(B)** As assessed by RT-qPCR, AAV6-BOLA3 increased BOLA3 transcript levels in CD31+ endothelial cells harvested from mouse lung. **(C-E)** As assessed by fluorescent microscopy, AAV6-BOLA3 increased lipoate (white, **C**) and GCSH (white, **D**) expression particularly in CD31+ endothelial cells **(E)**. **(F)** AAV6-BOLA3 delivery also decreased whole lung glycine content, as quantified by fluorometric assay. **(G-H)** As assessed by fluorescent microscopy,

AAV6-BOLA3 reduced PCNA **(G)** but enhanced cleaved caspase 3 (CC-3) expression **(H)** in both CD31+ and α-SMA+ cells in mouse pulmonary vessels. **(I-J)** AAV6-BOLA3 reduced pulmonary vessel thickness and muscularization, as assessed by hematoxylin and eosin as well as α-SMA staining. **(K-L)** AAV6-BOLA3 reduced right ventricular systolic pressure as measured by right heart catheterization but did not affect right ventricular hypertrophy (Fulton index, RV/LV+S). In panel B, mean expression of control group (AAV6-GFP) was normalized to fold change of 1, to which relevant samples were compared. Data represent the mean ± SEM (*P < 0.05, **P < 0.01, ***P < 0.001). Scale bars, 50μm. In these experiments, unless indicated otherwise, N = 8–10 mice/group.

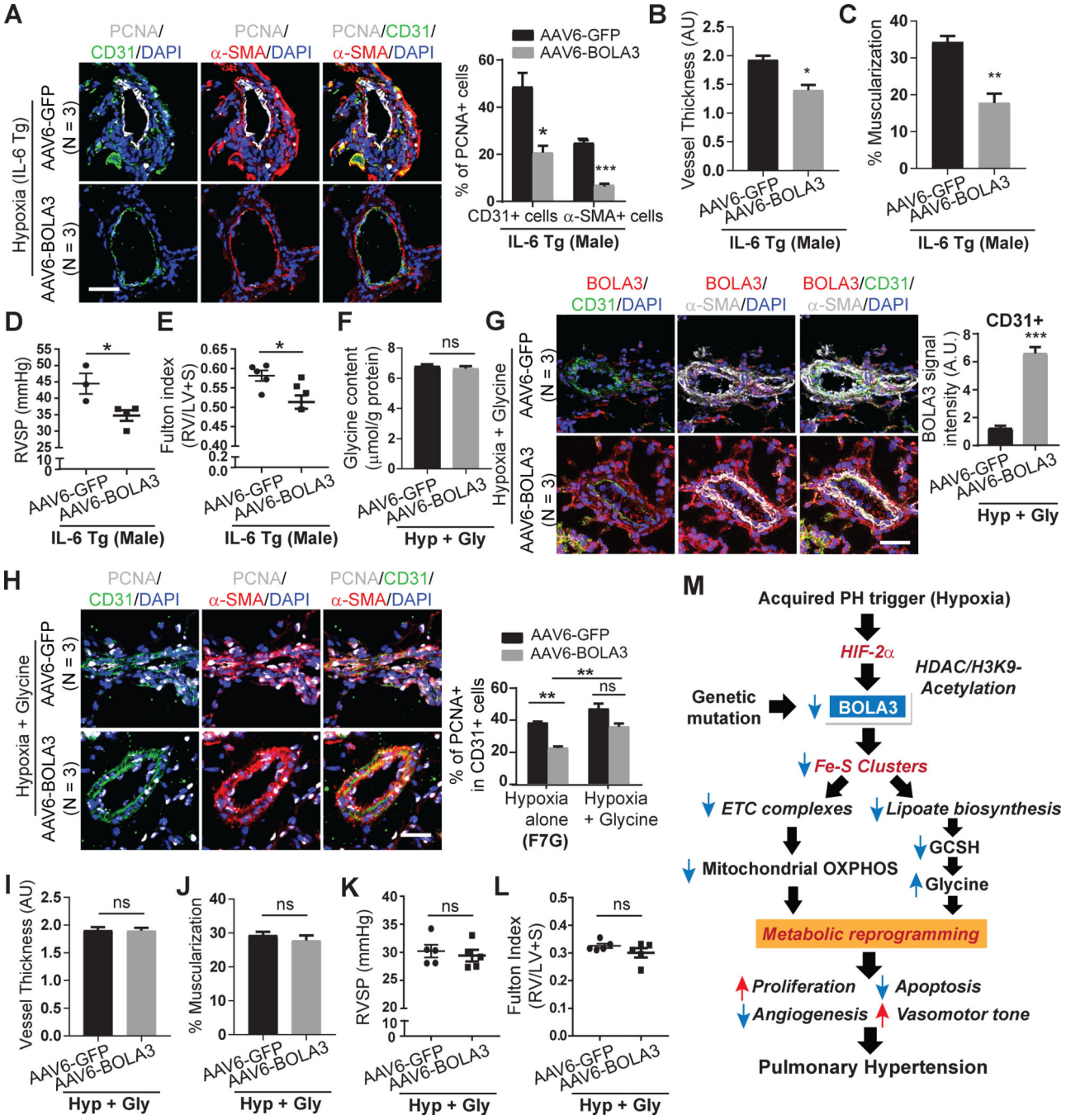

Figure 8: The therapeutic effects of BOLA3 in PH are reversed by a hyperglycinemic state.

(A) Similar to hypoxic wildtype mice, AAV6-BOLA3 reduced PCNA in CD31+ and α-SMA+ cells in pulmonary vessels of hypoxic IL-6 transgenic (IL-6 Tg mice). **(B-C)** In IL-6 Tg mice, AAV6-BOLA3 reduced pulmonary vessel remodeling. **(D-E)** In IL-6 Tg mice, AAV6-BOLA3 reduced right ventricular systolic pressure (RVSP) **(D)** and Fulton index **(E)**. **(F-G)** In hypoxic wildtype mice, as quantified by fluorometric assay, exogenous glycine prevented the ability of AAV6-BOLA3 to decrease lung glycine **(F)**, despite induction of BOLA3 in the pulmonary vasculature **(G)**. **(H)** Glycine maintained elevated PCNA in

pulmonary vascular CD31+ endothelial cells in hypoxic mice, despite BOLA3 expression. **(I-L)** Glycine prevented AAV6-BOLA3 from reducing pulmonary vessel remodeling **(I-J)** and from decreasing RVSP **(K)** or Fulton index **(L)** in hypoxic mice. Scale bars, 50μm; N = 3–5 mice per group. Data represent mean ± SEM (NS, $P > 0.05$, *$P < 0.05$, **$P < 0.01$, ***$P < 0.001$). **(M)** Model of BOLA3 deficiency in PH. BOLA3 is down-regulated genetically or epigenetically by hypoxia, decreasing [Fe-S] clusters and controlling electron transport and oxidative phosphorylation (OXPHOS). BOLA3 deficiency decreases lipoate biosynthesis, reducing the activity of 2-oxoacid dehydrogenases and further disrupting OXPHOS. Deficient lipoate biosynthesis also impairs glycine cleavage which promotes glycine retention and proliferation. This metabolic shift drives a proliferative, vasoconstricted vascular state, which predisposes to PH *in vivo*.